Geophys. J. R. astr. Soc. (1979) 59, 249–280

Seismic risk in southern Europe through to India examined using Gumbel's third distribution of extreme values

Paul W. Burton *Natural Environment Research Council, Institute of Geological Sciences, Murchison House, West Mains Road, Edinburgh EH9 3LA*

Received 1979 March 8; in original form 1978 September 19

Summary. A technique is described for the analysis of seismicity using Gumbel's third asymptotic distribution of extreme values. Seismicity of southern Europe through to India, nominally for the period 1900–74, is subdivided in a cellular manner, without recourse to tectonic discrimination between regions, and a covariance analysis on the three parameters of Gumbel's distribution is performed for each cell of seismicity. The results indicate that the upper bound to the magnitude of earthquake occurrence is often uncertain although it is discernible, while curvature of the earthquake occurrence distributions is usually established. Uncertainties in the forecasts of largest earthquakes, with a return period of 75 yr, are distinctly improved by taking into account the large and negative covariance which is measured between the curvature and upper bound to earthquake magnitude for the observed seismicity. These results are then used to map seismic risk for southern Europe through to India.

1 Introduction

The problem of assigning return periods to earthquake occurrences (earthquake or seismic risk) is fundamental to all investigations of seismic hazard and to most investigations of the characteristics of regional seismicity. Several statistical models have been applied to the analysis of earthquake occurrence sequences with varying degrees of success. Many of the results obtained are unsatisfactory because of undetected incompleteness in the data sets analysed or because even rudimentary studies into the inherent uncertainties associated with the parameters used to statistically describe the earthquake population are deemed to be of little consequence, or worse, omitted.

The most common description of earthquake occurrence is the cumulative frequency distribution, which relies on knowledge of all earthquake occurrence down to a particular magnitude threshold. Earthquake occurrence is described by:

$$\log N_c = a - bM \tag{1}$$

where N_c is the annual number of earthquakes with magnitude M or greater, a and b are constants. This effectively assigns the exponential distribution to describe earthquake occurrence. Within the European area this technique has been fully exploited by Kárník

(1968, 1971). The main disadvantages are that incompleteness in the magnitude data set can cause spurious results, and that this linear distribution does not attempt to describe the curvature observed at both high and low magnitude ranges. The second commonly used description of earthquake occurrence is the Poisson distribution which has been used to describe several seismic environments, including seismicity at the mid-Atlantic Ridge by Francis & Porter (1971).

The theory of extreme values described by Gumbel (1958) has the advantage that it does not require analysis of the complete record of earthquake occurrence, but uses the sequence of earthquakes constructed from the largest values of magnitude over a set of predetermined intervals. From equation (1) the annual extreme magnitude is seen to have the mean value a/b and clearly a description of earthquake occurrence which relies solely upon a sequence of annual extremes, rather than all earthquake occurrences, has certain attractions. It seems that extreme value statistics were first applied to seismic risk by Nordquist (1945), were reviewed by Lomnitz (1966) and more recently applied by Shakal & Willis (1972). Epstein & Lomnitz (1966) combined a distribution to describe the number of earthquake occurrences at a particular magnitude level with the frequency of earthquakes in a year, using the Poisson distribution. In this way they produced a model demonstrated to be the same as Gumbel's first asymptotic distribution of extreme values. This theory has been applied by Kárník & Hubnerova (1968) to estimate the probability of occurrence of largest earthquakes in the European area; it has subsequently been modified by Schenkova & Kárník (1970) to obtain the limiting earthquake at an infinite return period by using an hyperbolic extrapolation technique. Milne & Davenport (1969) extended the technique to observations of extreme intensities, Makjanic (1972) has applied Gumbel's third distribution of extreme values to the assessment of limiting intensities associated with Zagreb earthquakes and Yegulalp & Kuo (1974) have incorporated the method into the assessment of limiting earthquake magnitude on a global basis. Schenkova & Kárník (1974) have also compared alternative methods of determining largest possible earthquakes and Molchan, Keilis-Borok & Vilkovich (1970) have attempted to produce a statistical method for estimating the total effect of earthquakes, including damage.

This paper confines itself to a development in application of Gumbel's third asymptotic distribution of extreme values – Gumbel III – to the seismicity of southern Europe through to India. In particular the technique is developed so that the uncertainties in the parameters of the Gumbel III distribution are obtained and uncertainties in the prediction or forecasting of return periods associated with particular magnitude levels are assessed by means of the complete covariance matrix of errors in the distribution parameters.

The Gumbel III distribution includes a parameter which estimates the limiting largest earthquake magnitude possible in a region. However, the purpose of this paper, unlike Yegulalp & Kuo (1974), is not simply to estimate limiting magnitudes, although this is a by-product, but rather to obtain a good fit to earthquake occurrence histories so that subsequent prediction of occurrence will be improved. Secondly, the objective is to obtain adequate means of population estimation so that all parameters are well determined, or at least determined with a known precision. This line is pursued because the author believes it important that all statements of seismic risk should include some measure of the associated confidence limits, since the inherent economic consequences can only be estimated with a degree of known reliability if these statistics are included. This paper also adopts the procedure of dividing regional seismicity into simple cells (4° square), so that the analysis technique may be systematically applied. This lends itself to the production of seismic risk maps, giving the largest earthquake magnitude which may be expected in a region over a 75-yr interval.

2 Extreme value statistics

Following Nordquist's (1945) demonstration that the largest earthquakes in California are in agreement with the theory of extreme values, the theory has been used in other disciplines. For instance, Jenkinson (1955) and Gringorten (1963b) have analysed meteorological extremes, and Krumbein & Lieblein (1956) have analysed the distribution of unusually large boulders in gravel deposits.

The frequency distribution of the largest members of a sample has been discussed by Fisher & Tippett (1928), but the most complete description of extreme value statistics is the lengthy development by Gumbel (1958), which follows his previous work (Gumbel 1945) on the analysis of floods. Gumbel's theory may be summarized as follows. The probability function $F(X)$ of a random variable X is

$$F(X) = P(X \leqslant m), \tag{2}$$

but we are seeking extreme values of the variable X. If $F(X)$ is sampled then the probability that m is the extreme value obtained from n independent samples is given by

$$G(m) = P(X_1 \leqslant m, X_2 \leqslant m, \ldots X_n \leqslant m), \tag{3}$$

hence

$$G(m) = F^n(X). \tag{4}$$

If the parent population $F(X)$ is well defined, for example the Poisson distribution might be assumed, then the distribution $G(m)$ is also defined. Usually the parent distribution $F(X)$ is not known, but Gumbel demonstrated that: if $F(X)$ is *one* of the various exponential distributions, then $G(m)$ will be an asymptotic distribution of extremes of which there are three possibilities. The first of Gumbel's asymptotic distributions of extremes – Gumbel I – is given by

$$G^{\mathrm{I}}(m) = \exp\{-\exp[-\alpha(m-u)]\}. \tag{5}$$

This distribution has two parameters: α and the characteristic, or modal extreme, u. Epstein & Lomnitz (1966) have demonstrated the application of this cumulative frequency distribution to Californian earthquakes and they have established the general relationship between the parameters of equation (5) and the common cumulative frequency relationship expressed by equation (1). Gumbel's second asymptotic distribution is mentioned for completeness; this distribution has a lower limit to the range of extreme values and is not considered further here.

The third asymptotic distribution of extremes – Gumbel III – takes the form

$$G^{\mathrm{III}}(m) = \exp\left[-\left(\frac{w-m}{w-u}\right)^k\right]. \tag{6}$$

This three parameter distribution allows for curvature through the shape or curvature parameter k, it has an upper bound or limit w to the range of extreme values, and u is again the characteristic extreme value. It necessarily follows that $G^{\mathrm{III}}(w) = 1$ and $G^{\mathrm{III}}(u) = 1/e$.

Yegulalp & Kuo (1974) have used Gumbel III to predict the occurrence of maximum magnitude earthquakes. They point out that the occurrence of maximum magnitude earthquakes must have an upper bound, and hence the parameter w is of considerable importance. Many authors when plotting cumulative frequency distributions have noted 'roll-off' or curvature as the rarer high magnitude events are approached. Thus it does seem that Gumbel III is a more appropriate description of the natural phenomenon of earthquake occurrence. However, the parameters of Gumbel III which are obtained in this paper are not

sought just as an end in themselves, rather because the good fit to the data given by the complete distribution implies improved forecasting. In particular it is also clear that the upper magnitude parameter w will be approached from above as the data extent increases, even when it is determined with an unacceptably high value bracketed within wide ranging confidence limits.

If equations (5) or (6) are obtained using annual extremes then the return period $T(m)$ for the event m is given by

$$T(m) = \frac{1}{1 - G(m)}. \tag{7}$$

The prediction of the mode, median, or mean earthquake for a given return period is considered later.

3 Curve fitting technique and parameter estimation

It is relatively easy to estimate the parameters of either the cumulative frequency distributions of equation (1) or of Gumbel I defined in equation (5). Usually the procedure involves the least squares estimates of a and b in equation (1); for Gumbel I, equation (5) is expressed in terms of the reduced variate as

$$-\ln\,[-\ln G^{\mathrm{I}}(m)] = \alpha(m - u), \tag{8}$$

and again α and u are easily estimated. Both Aki (1965) and Utsu (1966) have pointed out that maximum likelihood estimates of a and b etc. are easily obtained in this linear situation and they prefer this approach. Here we shall consider the Gumbel III distribution only, and solely examine non-linear least squares methods of analysis to obtain estimates of the parameters. Yegulalp & Kuo (1974) describe three methods for estimating the parameters of Gumbel III: their first, the method of moments, and their second, which relies on an analysis using the largest magnitude, require that the earthquake magnitude series has no intervals for which extreme magnitudes are not available. This is seldom the case in practise. Their third method of least squares allows for the possibility that estimates of the extreme magnitudes might be missing in some time intervals.

The method to be used here is non-linear least squares based on the technique outlined by Levenberg (1944), and developed by Marquardt (1963). The application of this method is developed so that the uncertainty on each parameter of the distribution is estimated, and the complete covariance matrix or error matrix is obtained. The covariance matrix will later be shown to be of great value when Gumbel III is used for the prediction of earthquake occurrence at known confidence levels.

Equation (6) may be transposed to give m, using probability $P(m)$ to replace $G^{\mathrm{III}}(m)$, as

$$m = w - (w - u)\,[-\ln (P(m))]^{\lambda} \tag{9}$$

where $\lambda = 1/k$. The usual procedure for fitting a non-linear function $y(x)$ is to linearly expand $y(x)$ in a Taylor series function of parameters p_j and then perform linear least squares to obtain optimum values for perturbations δp_j to the initial trial values of p_j. This leads to

$$y(x) = y_0(x) + \sum_{j=1}^{r} \left[\frac{\partial y_0(x)}{\partial p_j}\,\delta p_j\right], \tag{10}$$

and if this function is fitted to the n observables y_i, the goodness of fit may be measured by

χ^2 with

$$\chi^2 = \sum \left\{ \frac{1}{\sigma_i^2} [y_i - y(x_i)]^2 \right\}, \tag{11}$$

where σ_i is the standard deviation associated with each data point. χ^2 is minimized with respect to each parameter in turn leading to the linear matrix equation

$$\mathbf{B} = \delta\mathbf{p} \cdot \mathbf{A}, \tag{12}$$

where the elements of **A** and **B** are given by

$$\left.\begin{aligned} A_{jk} &= \sum \left[\frac{1}{\sigma_i^2} \frac{\partial y_0(x_i)}{\partial p_j} \frac{\partial y_0(x_i)}{\partial p_k} \right], \\ \text{and} \\ B_k &= -\frac{1}{2} \frac{\partial \chi_0^2}{\partial p_k} = \sum \left\{ \frac{1}{\sigma_i^2} [y_i - y_0(x_i)] \frac{\partial y_0(x_i)}{\partial p_k} \right\}. \end{aligned}\right\} \tag{13}$$

The solution of equation (12) is

$$\delta\mathbf{p} = \mathbf{B}\mathbf{A}^{-1} = \mathbf{B}\boldsymbol{\epsilon} \tag{14}$$

where $\boldsymbol{\epsilon}$ is the symmetrical covariance, or error matrix. Using equation (9) as the fitting function requires three parameters p_1, p_2, p_3, which will be w, u and λ, respectively. The covariance matrix $\boldsymbol{\epsilon}$ of equation (14) is then of the form

$$\begin{pmatrix} \sigma_w^2 & \sigma_{uw}^2 & \sigma_{\lambda w}^2 \\ \sigma_{wu}^2 & \sigma_u^2 & \sigma_{\lambda u}^2 \\ \sigma_{w\lambda}^2 & \sigma_{u\lambda}^2 & \sigma_\lambda^2 \end{pmatrix}, \tag{15}$$

and from this the parameter uncertainties are obtained, as well as evidence of dependence between the parameters. Equation (10) includes the partial derivatives which from equation (9) are

$$\left.\begin{aligned} \frac{\partial m}{\partial w} &= 1 - (-\ln P)^\lambda, \\ \frac{\partial m}{\partial u} &= (-\ln P)^\lambda, \\ \text{and} \\ \frac{\partial m}{\partial \lambda} &= -[(w-u)(-\ln P)^\lambda \ln(-\ln P)]. \end{aligned}\right\} \tag{16}$$

Marquardt (1963) has suggested an algorithm for solving equation (12), which relies on increasing the diagonal elements of matrix **A** by a factor η. When η is large, off-diagonal terms are trivial, and the diagonal terms dominate, leading to the degeneration of equation (12) into separate equations

$$B_j \approx \eta \cdot \delta p_j \cdot A_{jj} \tag{17}$$

the solutions for δp_j are analogous to those obtained by a gradient search. When η is small the solution using the complete linearized matrix of equation (12) is obtained. Equation

(12) thus becomes

$$\mathbf{B} = \delta\mathbf{p} \cdot \mathbf{C}, \tag{18}$$

with

$$\left.\begin{matrix} C_{jk} = A_{jk}(1+\eta) \\ A_{jk} \end{matrix}\right\} \begin{matrix} j = k \\ j \neq k. \end{matrix} \tag{19}$$

This procedure is efficient, if η is carefully adjusted during the iterations, and Marquardt suggests a suitable iteration scheme. Eventually the value of η is decreased so that the final iterations approach as nearly as possible the analytic linearized solution which is dictated by equation (12). Several options are available for testing convergence. It is possible to fix the number of iterations, although this gives no information about the degree of convergence achieved. In practise values of w, u and λ were accepted here, when an F test showed the χ^2 generated by successive iterations was similar at the 95 per cent confidence level. The maximum number of iterations allowed is five, and usually three are sufficient. Elements of the covariance matrix in equation (15) are finally calculated when η is reduced to a very small value or zero.

4 The data

The primary information, from which the extreme values are obtained, consist of a large file of earthquake hypocentral data from which the magnitudes of earthquakes within a particular region are extracted. The initial collection of data was started in 1965 by Latter (1970), and continued by Lilwall. The present file of earthquake hypocentral data is described in detail by Burton (1978c), and published in Atlas form by Crampin *et al.* (1976). Since 1964 the principal reporting agency incorporated into the file is the International

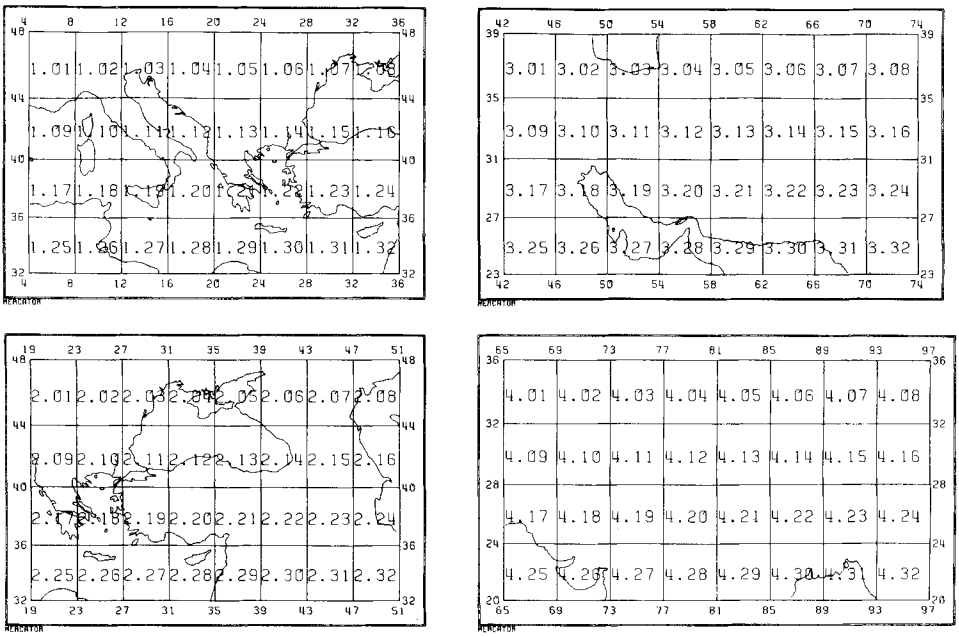

Figure 1. The four geographic regions used in the extreme value analysis are each subdivided into 4° cells. Reference to a particular cell in the text or tables is made through the cell code numbers shown in these diagrams.

Seismological Centre (ISC), and this is well supplemented by the Preliminary Determination of Epicentres (PDE) service of the US National Earthquake Information Service (NEIS). Added to these international agencies is the work of individual researchers, principally Gutenberg & Richter (1954), Kárník (1968, 1971) and Rothé (1969). Earthquake size is quantified on the surface wave magnitude scale, and in a small percentage of cases this has been achieved by converting a body wave magnitude to the corresponding point on the surface wave scale (Burton 1978c; Marshall 1970). Above magnitudes of around 5.5 the surface wave magnitude is commonly available and M_S is unlikely to be significantly depressed (Kanamori 1977, 1978) for earthquakes of Europe and the Middle East.

The four major geographic regions of Fig. 1 have been analysed, covering those parts of Europe with major seismic activity and extending through the Middle East. The United Kingdom is the subject of other work (Lilwall 1976; Burton 1978a) in which macroseismic data from historical earthquakes is incorporated to obtain an adequate extreme value population.

Each of these major regions may be conveniently partitioned into cells of 2, 4 or 8° side for specific data analyses, and a cell of 4° side is used here. A cell of 4° side is preferred because smaller cells mostly contain insufficient data for the statistical analysis, while larger ones clearly give poorer spatial resolution. Although this cellular structure is without exact tectonic consideration, many tectonic and seismic features are discernible on this scale. The cells vary in area for different latitudes, but the difference is small for the narrow latitude range considered and no allowance is made for this during the analysis.

The time span covered for each cell is, whenever possible, 1900 to 1974 inclusive. In practice it usually happens that the first available earthquake datum occurs after 1900 and that year is then taken as the first possible extreme datum.

5 Plotting points, weights and appropriate intervals for the extreme values

Once the cellular acquisition of the data has been achieved it is a simple matter to obtain a list of annual extremes, including 'missing' entries for those years with no known earthquake. After the extremes are ranked as in equation (3) a value has to be assigned to the probability function $P(m)$, individual extremes can be weighted and, when 'missing' extremes are present, the interval during which extremes are obtained has to be adjusted so that the number of actual extreme values is relatively significant when compared with the number of missing extremes.

5.1 'PLOTTING POINT'

The n annual extreme magnitudes m_i are arranged in ascending size, so that $m_1 \leqslant m_2 \leqslant m_3 \ldots \leqslant m_n$. Usually the 'plotting point' probability value at m_i is

$$P(m_i) = \frac{i}{(n+1)} \tag{20}$$

but Kimball (1960), Gringorten (1963a), and other authors have suggested alternatives such as

$$P(m_i) = (i - \tfrac{1}{2})/n, \tag{21}$$

$$P(m_i) = (i - \tfrac{3}{8})/(n + \tfrac{1}{4}), \tag{22}$$

or

$$P(m_i) = (i - 0.44)/(n + 0.12). \tag{23}$$

Formula (20) is usually accepted in geophysics. Jenkinson (1955) points out that equation (21) is a compromise between $(m-1)/n$ and m/n for the cumulative frequency of the mth point. Kimball (1960) discusses the problem of selecting suitable plotting points designed for particular purposes, for instance equation (22) may be appropriate when extrapolation to the right is required. Gringorten (1963a, b) suggests that equation (23) is most suitable for the double exponential Gumbel I distribution, and this is finally chosen for Gumbel III, because we are more interested in obtaining the best fit for high magnitudes and long return periods.

5.2 WEIGHTING THE EXTREMES

The reliability of earthquake monitoring and reporting has improved during this century and the weight attributed to each extreme datum should reflect this. Dividing this century into three periods gives block uncertainties in magnitude of:

Before 1915 $\delta m = 1.0$
1915–1954 $\delta m = 0.75$
after 1954 $\delta m = 0.5$.

This division is not to be interpreted as an exact transition in quality, but should be seen as a reflection of improvements, starting around 1915, with the widespread introduction of the Milne–Shaw seismometer and photographic recording, similarly the improvements from around 1954 follow the work of Gutenberg & Richter (1954), which brought about a more careful determination of magnitude, accompanied by a worldwide increase in the number of monitoring seismograph stations. There seems little to be gained from a more sophisticated weighting, whereas this schemes does represent improvements in the data and reduces the risk that large but possibly inaccurate magnitudes at the start of this century could bias the results.

5.3 EXTREME INTERVALS

A set of weighted annual extremes generally contains a number of missing entries, MISS, between the data for the first and last extreme earthquake. It is not necessary to use annual extremes because the interval during which extremes are extracted may be extended from one to NPER years. The distribution $P_{\mathrm{NPER}}(m)$ for NPER year intervals is related to $P_1(m)$ for the annual extremes by:

$$P_{\mathrm{NPER}}(m) = P_1^{\mathrm{NPER}}(m). \tag{24}$$

Return periods $T_{\mathrm{NPER}}(m)$ now relate to the number of extreme intervals, rather than the number of years for m to be exceeded, and it follows that

$$T_{\mathrm{NPER}}(m) \approx \frac{T_1(m)}{\mathrm{NPER}}. \tag{25}$$

Kárník & Hubnerova (1968) and Kárník & Schenkova (1978) filled 'missing' extremes by assuming a largest magnitude chosen to correspond to a peak central intensity, I_0 of V.

In this paper unobserved earthquakes are not invoked to assign values to the missing extremes, and any cell which has one quarter or more missing is rejected on the grounds that the data set is inadequate for reliable curve fitting. However, the number of missing extremes may be reduced by increasing NPER and this process will accommodate more cells.

Several procedures were tested spanning the use of annual extremes to incrementing NPER until there are no missing extremes. The procedure adopted as most satisfactory increments NPER in a cell until MISS ⩽ ¼ and then the cell parameters are determined.

Incrementing NPER and extending the period from which extreme values are selected in order to accommodate the configuration of missing data necessarily involves the deletion of what are acceptable extreme values for a lower order of NPER. This contributes to a reduction in precision and in some instances one observes $\sigma_w \approx w$. Many cells do not change in parameters w, u, λ, as the conditions are relaxed to allow less precise results; the relaxation of criteria by which cells are accepted principally affects those cells with sparse data. The adopted criterion of incrementing NPER until MISS ⩽ ¼ is found to be particularly useful in that it extends our knowledge of the upper limit w, and the distribution in general, into some of those cells which would otherwise be rejected. Results for the cell parameters and the associated covariance matrices are thus obtained for about 75 per cent of the 4° cells in the four major regions.

6 Gumbel III cell parameters, diagrams and covariance matrices

6.1 CELL PARAMETERS

Tables 1(a) to (d) list results of w, u and λ, with standard deviations for the 4° cells in the four major regions. All of these results are obtained using the criterion that NPER is incremented until MISS ⩽ ¼. Also listed in these tables is the number of earthquakes reported in each cell.

These tables of parameter values yield some general results. Characteristic values u are usually well determined for each cell whereas upper magnitudes w and curvatures λ generally show much greater uncertainty.

Table 1. (a) The estimates of Gumbel III parameters for each 4° cell within the major Region 1.

Cell		w	σ_w	u	σ_u	λ	σ_λ	NQ	NPER	MISS
1.01	44, 04	6.11	0.44	4.39	0.18	0.70	0.29	450	2	5
1.02	44, 08	5.57	0.34	4.59	0.12	0.71	0.24	668	1	0
1.03	44, 12	5.74	0.36	4.64	0.12	0.65	0.22	696	1	0
1.04	44, 16	6.83	0.94	4.26	0.10	0.32	0.17	368	1	8
1.05	44, 20	6.27	0.59	3.92	0.18	0.76	0.29	166	2	5
1.06	44, 24	7.62	1.95	4.98	0.17	0.33	0.35	255	2	6
1.09	40, 04	6.63	2.25	4.13	0.27	0.56	0.72	59	5	2
1.10	40, 08	5.65	0.40	3.51	0.14	0.81	0.30	224	1	16
1.11	40, 12	6.40	0.58	4.55	0.11	0.49	0.20	672	1	3
1.12	40, 16	6.74	1.11	4.90	0.11	0.36	0.28	801	1	5
1.13	40, 20	6.87	0.80	4.86	0.11	0.45	0.23	735	1	3
1.14	40, 24	7.38	1.11	4.73	0.17	0.52	0.30	326	2	3
1.15	40, 28	7.65	0.76	4.35	0.14	0.45	0.15	194	2	3
1.16	40, 32	7.25	0.65	4.39	0.19	0.77	0.32	110	2	7
1.17	36, 04	8.11	9.72	4.72	0.26	0.19	0.67	61	4	1
1.18	36, 08	7.58	29.95	4.53	0.30	0.12	1.37	16	5	1
1.19	36, 12	8.21	1.79	4.28	0.11	0.29	0.17	318	1	8
1.20	36, 16	7.05	2.13	4.43	0.12	0.28	0.30	278	1	14
1.21	36, 20	8.19	1.03	5.58	0.11	0.35	0.17	3177	1	1
1.22	36, 24	12.76	8.41	5.07	0.11	0.11	0.14	1420	1	7
1.23	36, 28	7.19	0.66	4.88	0.11	0.51	0.22	827	1	10
1.24	36, 32	6.40	0.62	4.72	0.17	0.67	0.33	99	2	3
1.25	32, 04	6.15	0.97	4.55	0.32	0.88	0.92	40	4	3
1.27	32, 12	5.65	1.83	4.79	0.59	0.80	2.23	13	15	0
1.29	32, 20	7.06	1.23	5.18	0.17	0.45	0.39	326	2	2
1.30	32, 24	10.63	10.39	5.23	0.11	0.12	0.27	797	1	7
1.31	32, 28	7.19	0.62	4.39	0.16	0.73	0.29	227	2	8
1.32	32, 32	6.59	0.85	4.29	0.18	0.66	0.39	183	2	5

Cell: each 4° cell is identified by the coordinate of its south-west corner.
NQ: the number of earthquake reports for the cell.
NPER: the extreme interval, years.
MISS: the number of extreme intervals for which no earthquakes are reported.

Table 1. (b) The estimates of Gumbel III parameters for each 4° cell within the major Region 2.

Cell	w	σ_w	u	σ_u	λ	σ_λ	NQ	NPER	MISS
2.01 44, 19	5.65	0.38	4.25	0.18	0.95	0.39	213	2	4
2.02 44, 23	7.31	1.07	4.29	0.13	0.39	0.21	240	1	17
2.03 44, 27	6.05	1.25	4.68	0.41	0.94	1.34	37	7	1
2.09 40, 19	7.05	1.22	4.99	0.10	0.30	0.23	906	1	2
2.10 40, 23	9.38	2.86	4.32	0.14	0.24	0.17	379	1	15
2.11 40, 27	7.24	0.87	4.75	0.18	0.63	0.32	235	2	4
2.12 40, 31	7.33	0.59	4.30	0.19	0.80	0.28	130	2	7
2.13 40, 35	7.73	1.02	5.06	0.24	0.59	0.31	69	4	1
2.14 40, 39	8.13	2.08	4.24	0.20	0.37	0.29	94	2	8
2.15 40, 43	6.11	0.47	4.59	0.13	0.68	0.37	282	1	13
2.16 40, 47	6.66	0.68	4.74	0.15	0.54	0.33	144	2	6
2.17 36, 19	8.02	0.99	5.44	0.11	0.34	0.17	2760	1	1
2.18 36, 23	9.21	2.23	5.17	0.11	0.25	0.17	1639	1	6
2.19 36, 27	8.34	1.34	5.07	0.11	0.31	0.17	1119	1	8
2.20 36, 31	6.70	0.90	4.15	0.16	0.58	0.33	109	2	8
2.21 36, 35	10.47	7.02	4.94	0.15	0.16	0.23	132	2	3
2.22 36, 39	7.28	0.69	5.13	0.16	0.54	0.29	254	2	6
2.23 36, 43	7.71	2.10	4.72	0.15	0.30	0.28	165	2	4
2.24 36, 47	6.66	3.14	4.61	0.18	0.37	0.75	78	3	3
2.25 32, 19	7.22	2.08	4.81	0.23	0.43	0.56	185	3	4
2.26 32, 23	7.09	0.71	5.17	0.11	0.51	0.27	713	1	9
2.27 32, 27	7.16	0.73	4.48	0.13	0.50	0.23	425	1	17
2.28 32, 31	6.95	1.82	4.90	0.23	0.59	0.72	108	3	3
2.29 32, 35	6.36	1.51	3.86	0.18	0.39	0.35	140	2	6
2.31 32, 43	5.76	1.32	4.98	0.23	0.63	1.74	77	3	3
2.32 32, 47	11.35	13.13	5.20	0.27	0.18	0.46	206	4	3

Table 1. (c) The estimates of Gumbel III parameters for each 4° cell within the major Region 3.

Cell	w	σ_w	u	σ_u	λ	σ_λ	NQ	NPER	MISS
3.01 35, 42	6.71	1.31	4.72	0.16	0.41	0.39	171	2	5
3.02 35, 46	6.91	1.06	4.50	0.19	0.48	0.35	88	3	5
3.03 35, 50	7.24	0.67	4.75	0.21	0.72	0.34	92	3	3
3.04 35, 54	8.68	3.36	4.88	0.22	0.30	0.37	174	3	4
3.05 35, 58	7.43	2.92	4.78	0.25	0.34	0.55	102	4	3
3.06 35, 62	7.14	1.82	4.71	0.38	0.71	0.83	20	8	1
3.07 35, 66	7.40	1.23	4.91	0.20	0.60	0.53	342	2	6
3.08 35, 70	7.65	0.36	5.88	0.11	0.72	0.24	1683	1	9
3.09 31, 42	5.70	2.16	4.96	0.47	0.61	2.24	20	10	0
3.10 31, 46	6.85	1.21	4.87	0.22	0.59	0.65	229	2	7
3.11 31, 50	7.25	1.51	4.51	0.35	0.61	0.58	62	4	3
3.12 31, 54	6.80	1.86	4.77	0.30	0.52	0.78	58	4	3
3.13 31, 58	9.63	10.85	5.25	0.28	0.18	0.58	74	6	2
3.15 31, 66	7.79	2.07	4.94	0.32	0.49	0.59	84	7	1
3.16 31, 70	6.98	101.24	4.86	0.25	0.08	4.21	111	4	3
3.19 27, 50	10.88	21.45	5.00	0.17	0.08	0.34	295	2	5
3.20 27, 54	7.33	0.92	5.08	0.27	0.67	0.55	315	3	5
3.21 27, 58	6.90	0.61	4.82	0.24	0.85	0.44	32	4	2
3.22 27, 62	8.84	1.68	4.76	0.32	0.58	0.38	23	5	2
3.23 27, 66	8.68	4.01	4.69	0.28	0.29	0.42	181	3	5
3.24 27, 70	8.42	94.59	4.96	0.39	0.11	3.36	43	9	1
3.27 23, 50	7.04	59.82	5.30	0.34	0.10	3.81	37	11	0
3.28 23, 54	6.09	0.61	4.45	0.20	0.50	0.69	75	3	5
3.29 23, 58	8.39	1.80	4.74	0.32	0.57	0.42	19	5	1
3.30 23, 62	7.93	1.29	5.48	0.36	0.77	0.64	56	9	1
3.31 23, 66	6.87	5.57	5.07	0.35	0.28	1.02	31	8	0
3.32 23, 70	6.86	2.96	5.06	0.44	0.45	0.93	9	13	0

6.2 CELL DIAGRAMS

It is useful to look at individual cells in greater detail and a graphical representation is helpful.

6.2.1 Generalized diagrams of Gumbel III

Statistically, the third asymptote is usually represented through the reduced variate $z = (w - m)/(w - u)$, and $\ln z$ is plotted against $-\ln(-\ln P)$ producing a straight line of gradient

Table 1. (d) The estimates of Gumbel III parameters for each 4° cell within the major Region 4.

Cell	w	σ_w	u	σ_u	λ	σ_λ	NQ	NPER	MISS
4.01 32, 65	7.96	2.84	5.28	0.34	0.49	0.71	46	11	0
4.02 32, 69	9.97	5.60	5.10	0.21	0.23	0.31	260	2	6
4.03 32, 73	7.44	2.34	4.78	0.36	0.58	1.04	146	4	3
4.04 32, 77	6.98	1.85	4.91	0.30	0.47	0.73	83	3	5
4.05 32, 81	8.37	3.91	4.94	0.29	0.34	0.50	32	5	1
4.06 32, 85	9.56	15.27	4.92	0.37	0.21	0.87	39	7	1
4.07 32, 89	9.36	18.09	5.01	0.28	0.16	0.80	36	4	3
4.09 28, 65	8.00	2.44	5.17	0.24	0.47	0.58	114	4	2
4.10 28, 73	7.14	1.98	4.65	0.19	0.32	0.38	125	3	4
4.11 28, 73	7.12	2.48	4.58	0.42	0.58	0.83	26	9	1
4.12 28, 77	7.90	1.24	4.72	0.27	0.56	0.40	93	3	5
4.13 28, 81	8.52	12.04	4.75	0.26	0.15	0.60	87	3	5
4.14 28, 85	7.20	1.80	4.59	0.34	0.56	0.58	52	5	2
4.15 28, 89	8.64	2.06	4.92	0.22	0.38	0.32	84	3	4
4.16 28, 93	8.30	2.03	4.99	0.27	0.51	0.48	176	6	2
4.17 24, 65	6.49	5.26	4.83	0.57	0.60	3.32	60	4	3
4.22 24, 85	8.35	2.83	4.45	0.30	0.41	0.41	36	4	1
4.23 24, 89	7.29	0.64	4.80	0.22	0.78	0.40	123	2	7
4.24 24, 93	8.02	0.70	5.47	0.17	0.55	0.28	218	2	7
4.32 20, 93	10.56	6.15	4.93	0.21	0.22	0.31	125	2	5

$-\lambda$. Fig. 2(a) shows a plot similar to the statistical convention. Fig. 2(b) shows the same Gumbel parameter suite with the curves drawn in a manner more familiar in seismology with m against $-\ln(-\ln P)$. Both Figs 2(a) and (b) tend to stress the effect of the curvature parameter, which, although of importance, does not have the immediate consequences of either the characteristic magnitude or the upper magnitude limit. Fig. 2(b) indicates the asymptotic approach to the upper magnitude limit, and the cross over point for all λ at the characteristic magnitude u where $-\ln(-\ln P) = 0$. Fig. 2(a) obscures these properties by plotting $\ln(w - m)$ as ordinate, but neither the representation of Fig. 2(a) nor Fig. 2(b) readily lends itself to seismological interpretation.

Fig. 2(c) is designed to stress w and u, at the expense of λ, for ease of interpretation, and to bear analogy with the more familiar cumulative frequency distribution of equation (1). Rearranging equation (6) gives

$$m = w - (w - u)\,[-\ln(P(m))]^{\lambda}, \tag{26}$$

and so Fig. 2(c) has gradient $-(w - u)$ with intercept w and the abscissa is scaled to $(-\ln P(m))^{\lambda}$. Over the 90 per cent probability range 0.05 to 0.95 the projection of the line onto the abscissa, for λ varying from 0.5 to 0.1, scales the abscissa by a factor of about 4. The annual earthquake, or annual extreme value, in the cumulative frequency equation (1) is a/b and this may be compared with the characteristic magnitude u. The value of $(w - u)$ for Fig. 2(c) indicates how rapidly the seismicity falls off from the upper magnitude limit.

6.2.2 Particularized cell diagrams of Gumbel III

In the ensuing graphs, the data for each successful cell are superimposed onto the theoretical line obtained from the cell parameters. Deviations of the data from the straight line can be divided into four categories, each of which is indicated by the hypothetical dotted lines, numbered 1 to 4 on Fig. 2(c). Briefly, these data deviations from the ideal straight line may indicate for such a cell that:

Arm 1: The probability of a large magnitude being an extreme is observationally lower than presently predicted by the theoretical line.

Arm 2: This is the converse of Arm 1. Observationally these magnitudes are assigned a

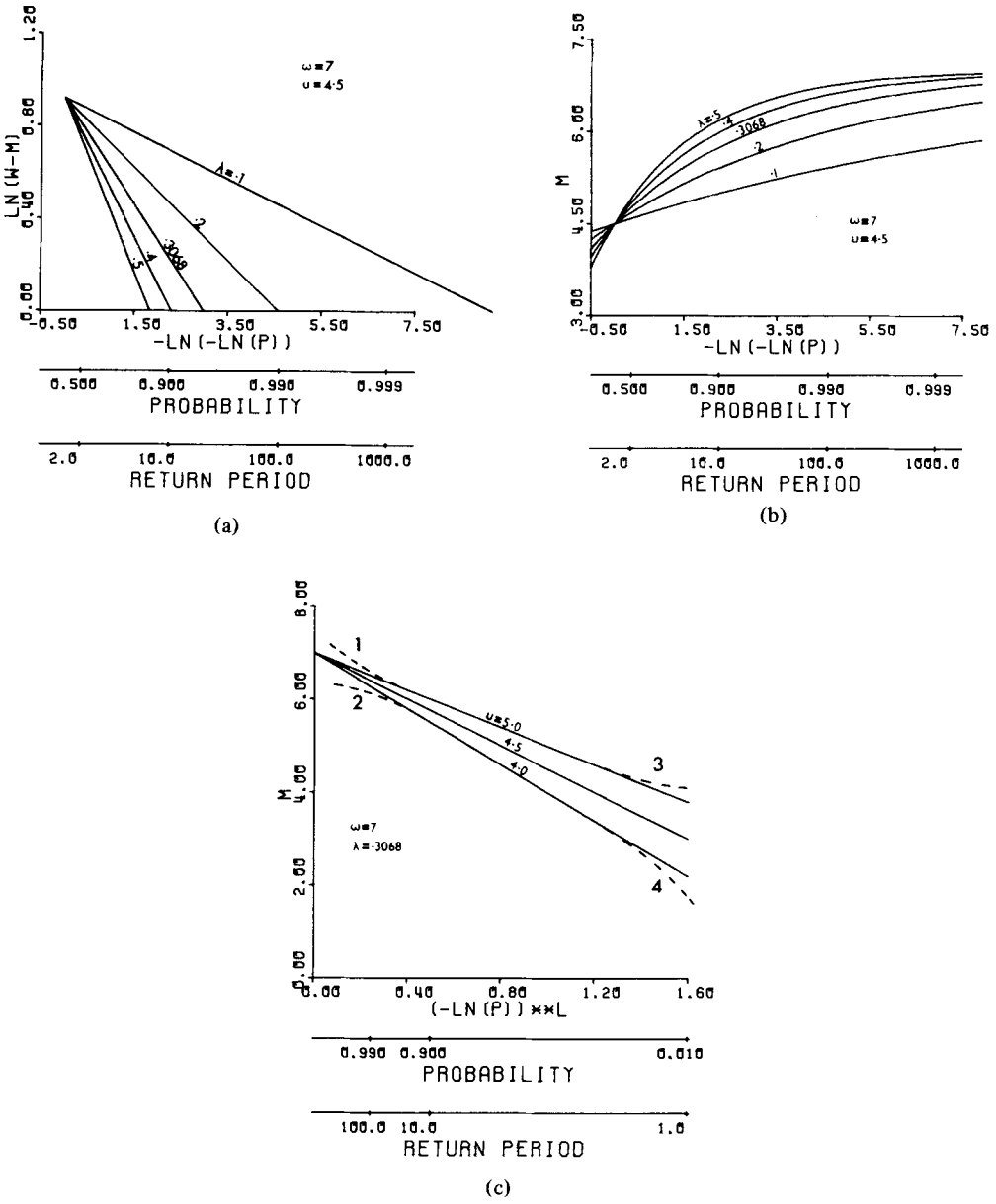

Figure 2. (a) The standard statistical representation of the Gumbel III asymptotic distribution of extreme values with the reduced variate $\ln(w - m)$ plotted against the function $-\ln(-\ln P)$ of the probability P. Gumbel III parameters used are $w = 7$, $u = 4.5$ and $\lambda = 0.1$, 0.2, 0.3068, 0.4, 0.5. For $\lambda = 0.3068$ the median and modal values of the distribution are equal. The subsidiary axes denote both the probability P that a magnitude m earthquake is an extreme value and also its return period T in years (annual extreme values are assumed). Large values of λ imply a rapid fall-off from the upper bound to magnitude w. (b) The standard geophysical representation of Gumbel III with magnitude m plotted against the function $-\ln(-\ln P)$ of the probability P. Gumbel III parameters used are $w = 7$, $u = 4.5$, $\lambda = 0.1$, 0.2, 0.3068, 0.4, 0.5. The cross-over occurs with $m = u$ at $P = 1/e$. (c) Plots of m against $(-\ln P)^{\lambda}$ with Gumbel III parameters set at $w = 7$, $\lambda = 0.3068$ and u running through 4.0, 4.5, 5.0. This is the preferred representation of Gumbel III and is used throughout this paper. The dotted lines, arms numbered 1 to 4, indicate possible deviations of the observational data from the ideal linear case and are discussed in the text.

probability of being an extreme which is probably an overestimate. (An alternative explanation, which can merit investigation, is that these magnitudes are underestimated, and the converse of this applies to Arm 1.)

Arm 3: The probability of being an extreme m is observed to be lower than the line predicts or the extreme magnitudes are being overestimated. This situation might arise through inhomogeneity, or alternatively, a local earthquake swarm might bias the probability estimates to smaller values than would normally be the case for independent extremes.

Arm 4: This situation might imply that the magnitude values used as extremes for this arm of the distribution are significantly below the threshold of completeness, and therefore are assigned too large a probability of being extreme values. It is also possible that inhomogeneity in reporting smaller magnitudes may introduce a systematic underestimate of the magnitudes in this arm. This may arise because estimates of smaller magnitudes rely mainly on local reporting stations.

These interpretations are useful for several cells, but should not be taken as absolute guidance because such data deviations must also be subject to statistical scatter around the derived distribution. Diagrams based on Fig. 2(c) are produced as small sketches for every cell of each region in Figs 3(a–d).

6.3 DISCUSSION OF RESULTS FOR THE INDIVIDUAL CELLS

Covariance matrices associated with each cell are described and tabulated in a later section. A combination of the above general guide, the cell diagrams and the covariance matrices will usually be sufficient to interpret the results from each cell. Some specimen cells, mainly selected from Region 1, are now described in detail.

Central Italy is covered by cell 1.11 in Fig. 3(a). Table 1(a) shows that there is a large earthquake population, 672 earthquakes, and that annual extremes could be extracted leaving only three missing intervals, leading to cell parameters which are well determined with very small standard deviations. Inspection of the cell diagram shows that the ensuing theoretical fit to the data is visually good. There is a slight tendency to show an 'Arm 1' type of deviation at the higher magnitude extremes, which, if not statistical scatter, could indicate that, for instance, the magnitude 7 earthquake of 1915 January 13, is overestimated by Gutenberg & Richter (1954). Cell 1.21 covers most of Greece and this yields similar results, although the magnitudes are higher. The largest extreme value for this cell is magnitude 8.3 which could also be overestimated. Directly east of Greece is western Turkey, cell 1.22, which, although it has a large earthquake population, produces results with a high w accompanied by high uncertainty. However, the value of λ is very low, indicating little curvature, and implying that the earthquake occurrence distribution is linear up to high magnitudes, and that the present data set shows no great tendency to a statistical upper limit. This uncertainty for w does not indicate that it is incorrect, but rather that this cell is not strongly exhibiting this characteristic. Furthermore this helps demonstrate that upper magnitude limits need not be sought as an end in themselves but rather as one parameter in the best statistical fit to the observed distribution.

Unfortunately the results for a few cells must be regarded as doubtful for one of several possible reasons. In cells 1.01, 02 and 03 are some of the few instances when several earthquakes are assigned a magnitude of 5 as reasonable when the contemporary ISS list does not detail magnitude. Cell 1.27 invokes 15 yr extremes and cell 1.18 shows a visually poor fit to the data arising when iteration caused no significant improvement in χ^2; in both cases there are too few degrees of freedom. Extending the extreme interval beyond 2 yr increases

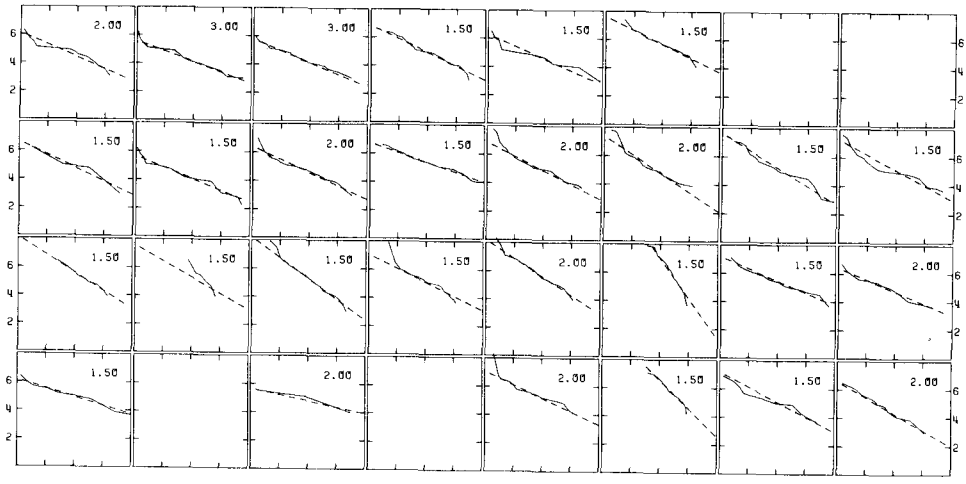

(a)

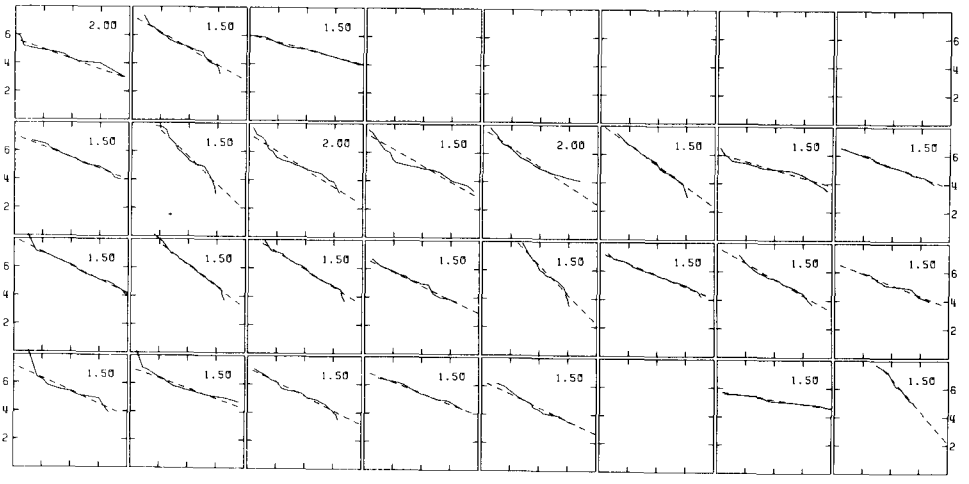

(b)

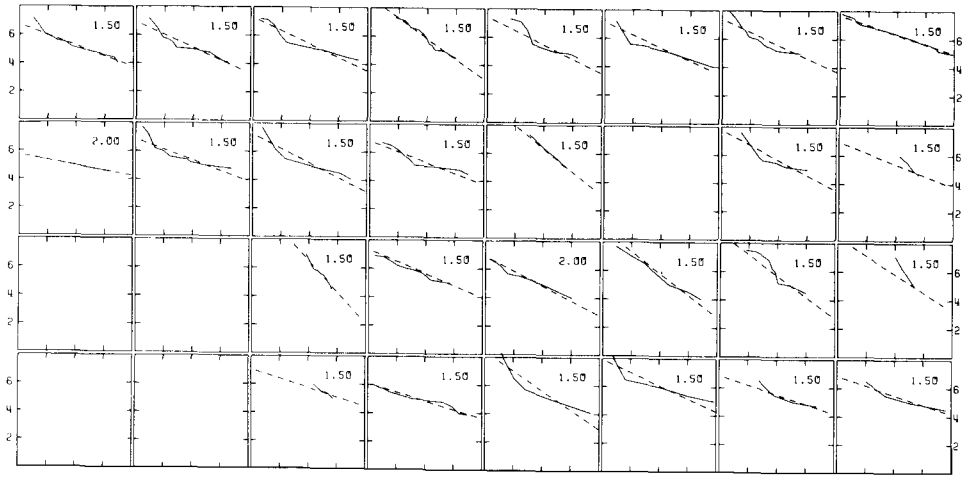

(c)

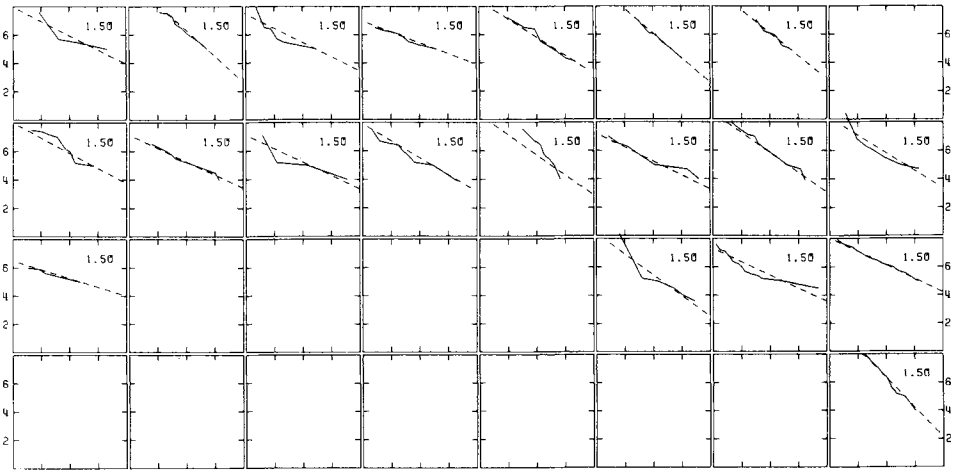

(d)

Figure 3. The data (solid line) and the Gumbel III fit to the data (dotted line) are plotted for each 4° cell which is specified by the coordinates of its south-west corner. The format of these diagrams is discussed in detail in the text, and Fig. 2(c) is an enlarged and generalized version of these smaller cell diagrams. For every cell the ordinate is scaled equally and measures the surface wave magnitude M_S. The abscissae may be scaled differently from cell to cell and the complete length of the abscissa represents the quantity of $(-\ln P)^{\lambda}$ numbered in the top right of each cell diagram. These cell diagrams are positionally arranged to match their relative geographic positions shown in Fig. 1. (a) Gumbel III 4° cell diagrams for Region 1. (b) Gumbel III 4° cell diagrams for Region 2. (c) Gumbel III 4° cell diagrams for Region 3. (d) Gumbel III 4° cell diagrams for Region 4.

the number of cells with parameter estimates from 23 to 28. All the remaining cells are adequately described by the diagrams and parameter tabulations.

The second region pushes the analysis further east and, by overlapping the first region, allows a check on the stability of cell estimates. Cell 2.31 has several extreme magnitudes assigned as 5 and cell 2.03 is determined with few degrees of freedom. Of the 26 cells listed in Table 1(b) seven are obtained by extending the extreme interval beyond 2 yr.

Analysis of Regions 1 and 2 produces most satisfactory results, whereas the eastward extension into Regions 3 and 4, although useful, is less satisfactory. Relaxing the extreme interval beyond two years for Regions 3 and 4 increased the number of acceptable cells from 5 and 4 to 27 and 20 respectively. Any cell parameters determined using NPER greater than 5 should be viewed with caution. Cell diagrams using small λ, for example cell 3.16, are no longer diagnostically helpful because the data range is excessively shrunk when scaled by such small powers (in this case $\lambda \approx 0.08$). Unreliable cells include those for which data is sparse and not available until the 1920's and those where several extremes have been arbitrarily set to magnitude 5: cell parameters for 3.07, 16, 28, 29 and 4.03, 05, 10, 13, 22, 32 should be regarded as tentative at this stage. Despite these considerations, the other cell parameters in these two regions are good determinations without obvious defects.

6.4 STATISTICAL STABILITY OF CELL RESULTS

Overlapping sections between Regions 1 and 2 allows assessment of stability in the results. The overlap is staggered so that half of the cells overlap with three quarters of the area of a cell common to two separate determinations of the parameters. It is unlikely that the gross picture of seismicity which we are trying to discern will resolve seismicity variations of

Table 2. Gumbel III stability (independent estimates of w are compared for those cells of Regions 1 and 2 which overlap by three quarters of their area).

Cell Number Region 1/Region 2	w_1/w_2	Cell Number Region 1/Region 2	w_1/w_2
1.05/2.01	1.11	1.21/2.17	1.02
1.06/2.02	1.04	1.22/2.18	1.39
1.07/2.03	-	1.23/2.19	.87
1.08/2.04	-	1.24/2.20	.96
1.13/2.09	.97	1.29/2.25	.99
1.14/2.10	.79	1.30/2.26	1.49
1.15/2.11	1.07	1.31/2.27	1.004
1.16/2.12	.99	1.32/2.28	.96

$1 \times 4^\circ$ size, unless a particularly dominant tectonic feature is localized and bounded within the quarter cell which is not shared. In general we expect variations between overlapping cells only to reveal small graduations in the gross seismicity. Table 2 compares the results using w which is particularly liable to fluctuate, and it is quite clear that a high degree of stability has been achieved. The disparity measured by $w1/w2$ is less than about 5 per cent in the majority of cases. In three cases the disparity is greater than 20 per cent, usually because the parameter w is not well established in one or both cells. When this is the case, $u1/u2$ indicates a disparity of only 2 per cent for comparisons 1.22/2.18 and 1.30/2.26. For 1.14/2.10 the disparity in $u1/u2$ is about 10 per cent and this may indicate a genuine transition in seismicity phenomena between western Bulgaria and the land adjacent to the south-west corner of the Black Sea in European Turkey and Eastern Bulgaria.

The appearance of overlapping cell diagrams also confirms this stability. Greek earthquakes are shared by the cells 1.21 and 2.17 and the cell diagrams (Figs 3(a) and (b)) show almost identical characteristics. Other similar examples can be found by examining the cell diagrams.

6.5 COVARIANCE OR ERROR MATRICES

Equation (14) defines the covariance matrix ϵ which is expanded into elements appropriate to this paper in equation (15). Tabulated standard deviations of the cell parameters are obtained from the diagonal elements, and these should be included in any earthquake risk analysis. The matrix ϵ is tabulated in Figs 4(a) to 4(d) for each cell of each region, and these cell matrix diagrams are in the same order as the cell diagrams in Fig. 3. Each of these covariance values, including the off-diagonal terms, is used in, and important to, the earthquake risk predictions of the next section.

These matrices immediately yield results. Of all the terms, σ_w^2 is by far the largest with the natural implication that the upper limit to earthquake magnitude is often either difficult to measure with small uncertainty, or, in some instances, is not a well established phenomenon. The smallest diagonal term is σ_u^2; consequently the characteristic value u is the most precisely known parameter. This is reasonable because u has the probability of occurrence $1/e$ during any extreme interval, and so with several extreme intervals in a single data set, u is well constrained. The last diagonal term σ_λ^2, although numerically small is often of similar size to λ. Both curvature and the upper magnitude limit are difficult to resolve with high precision. Off-diagonal covariance terms give important information. Yegulalp

& Kuo (1974) noted correlation between w and λ and the matrix diagrams here show that a significantly large and negative covariance is usually measured for $\sigma^2_{w\lambda}$. Of the other two off-diagonal covariances, σ^2_{wu} is small and negative while $\sigma^2_{u\lambda}$ is small and positive, usually $|\sigma^2_{u\lambda}|$ is less than $|\sigma^2_{wu}|$. The matrix corresponding to cell 1.19 (Fig. 4(a)) is an example of all these points, and several other such typical results could easily be identified.

The implications are clear. u is the only independent parameter of Gumbel III, whereas w and λ are dependent. It is difficult to determine upper limits w with great accuracy. Hence, when upper limits are quoted, a knowledge of associated uncertainty is essential. Moreover, any prediction of earthquake return periods using Gumbel III should incorporate a knowledge of $\sigma^2_{w\lambda}$.

In practice, when the data in one cell show little curvature, and a high value of w, this will often be accompanied by large uncertainties in these parameters. This situation usually occurs when the time span of data in a cell proves insufficient to establish non-linear curvature (if it exists). It also implies the fortunate result that the limiting magnitude w will be conservatively approached from above, as the data base extends, and enhances precision in the distribution parameters.

It is unlikely that the values of limiting magnitudes are depressed by saturation of the M_s scale described by Chinnery & North (1975) and Kanamori (1977, 1978) because few of the extreme value sequences obtained contain many great earthquakes with M_s in excess of 8. Kanamori demonstrated that saturation of M_s and underestimation of earthquake energy occurs particularly for great earthquakes in the circum-Pacific belt.

7 Statistical prediction or forecasting

To indicate variations in earthquake risk, 75-yr earthquakes, $m(75)$, will be predicted. This corresponds to the nominal data span for each cell. Because prediction without any indication of uncertainty is of little value the data contained in the covariance matrices is incorporated into the method, and $m(75) \pm \sigma_m$ is obtained where σ_m is one standard deviation.

Because Gumbel III can be skew, the modal, median, mean value of $m(75)$, or the value predicted directly from equation (9), the 'return period value', may all be different. The probability density function of $P(m)$ is $\Phi(m)$, and $\Phi(m)$ is required for predictions over N extreme intervals, giving

$$\Phi(m) = Nk\left(\frac{w-m}{w-u}\right)^{k-1} P(m). \tag{27}$$

The modal value ($d\Phi(m)/dm = 0$) is:

$$m_1 = w - (w-u)\,[(1-\lambda)/N]^{\lambda}, \tag{28}$$

and the median (m_2) and mean (m_3) values can be obtained as

$$m_2 = w - (w-u)\,[-1/N \cdot \ln(0.5)]^{\lambda}, \tag{29}$$

and

$$m_3 = w - (w-u)\,(1/N)^{\lambda}\Gamma(1+\lambda), \tag{30}$$

where Γ represents the gamma function. The return period estimate from equation (9) is designated m_4. It is clear that m_1, m_2, m_3 and m_4 may differ significantly when short prediction lengths are required, although this will depend on the curvature λ, but for increasing N all four estimates converge to similar values. It is not crucial which statistic is chosen to

$$
\begin{bmatrix} 0.19 & -0.03 & -0.11 \\ -0.03 & 0.02 & 0.02 \\ -0.11 & 0.02 & 0.09 \end{bmatrix}
\begin{bmatrix} 0.11 & -0.02 & -0.07 \\ -0.02 & 0.01 & 0.02 \\ -0.07 & 0.02 & 0.06 \end{bmatrix}
\begin{bmatrix} 0.13 & -0.02 & -0.07 \\ -0.02 & 0.01 & 0.02 \\ -0.07 & 0.02 & 0.05 \end{bmatrix}
\begin{bmatrix} 0.88 & -0.02 & -0.15 \\ -0.02 & 0.01 & 0.00 \\ -0.15 & 0.00 & 0.03 \end{bmatrix}
\begin{bmatrix} 0.35 & -0.06 & -0.16 \\ -0.06 & 0.03 & 0.03 \\ -0.16 & 0.03 & 0.09 \end{bmatrix}
\begin{bmatrix} 3.79 & 0.00 & -0.66 \\ 0.00 & 0.03 & -0.01 \\ -0.66 & -0.01 & 0.12 \end{bmatrix}
\begin{bmatrix} \\ \\ \\ \end{bmatrix}
\begin{bmatrix} \\ \\ \\ \end{bmatrix}
$$

$$
\begin{bmatrix} 5.07 & -0.20 & -1.55 \\ -0.20 & 0.07 & 0.06 \\ -1.55 & 0.06 & 0.51 \end{bmatrix}
\begin{bmatrix} 0.16 & -0.01 & -0.11 \\ -0.01 & 0.02 & 0.01 \\ -0.11 & 0.01 & 0.09 \end{bmatrix}
\begin{bmatrix} 0.33 & -0.03 & -0.11 \\ -0.03 & 0.01 & 0.01 \\ -0.11 & 0.01 & 0.04 \end{bmatrix}
\begin{bmatrix} 1.23 & -0.05 & -0.31 \\ -0.05 & 0.01 & 0.01 \\ -0.31 & 0.01 & 0.08 \end{bmatrix}
\begin{bmatrix} 0.64 & -0.04 & -0.18 \\ -0.04 & 0.01 & 0.01 \\ -0.18 & 0.01 & 0.05 \end{bmatrix}
\begin{bmatrix} 1.23 & -0.07 & -0.31 \\ -0.07 & 0.03 & 0.02 \\ -0.31 & 0.02 & 0.09 \end{bmatrix}
\begin{bmatrix} 0.58 & -0.05 & -0.11 \\ -0.05 & 0.02 & 0.01 \\ -0.11 & 0.01 & 0.02 \end{bmatrix}
\begin{bmatrix} 0.42 & -0.02 & -0.19 \\ -0.02 & 0.03 & 0.01 \\ -0.19 & 0.01 & 0.10 \end{bmatrix}
$$

$$
\begin{bmatrix} 94.6 & -0.54 & -6.41 \\ -0.54 & 0.07 & 0.03 \\ -6.41 & 0.03 & 0.44 \end{bmatrix}
\begin{bmatrix} 896.9 & -0.47 & -40.8 \\ -0.47 & 0.09 & 0.01 \\ -40.8 & 0.01 & 1.87 \end{bmatrix}
\begin{bmatrix} 3.20 & -0.06 & -0.30 \\ -0.06 & 0.01 & 0.01 \\ -0.30 & 0.01 & 0.03 \end{bmatrix}
\begin{bmatrix} 4.52 & 0.00 & -0.63 \\ 0.00 & 0.01 & 0.00 \\ -0.63 & 0.00 & 0.09 \end{bmatrix}
\begin{bmatrix} 1.06 & -0.05 & -0.17 \\ -0.05 & 0.01 & 0.01 \\ -0.17 & 0.01 & 0.03 \end{bmatrix}
\begin{bmatrix} 70.8 & 0.01 & -1.17 \\ 0.01 & 0.01 & 0.00 \\ -1.17 & 0.00 & 0.02 \end{bmatrix}
\begin{bmatrix} 0.43 & -0.03 & -0.14 \\ -0.03 & 0.01 & 0.01 \\ -0.14 & 0.01 & 0.05 \end{bmatrix}
\begin{bmatrix} 0.39 & -0.05 & -0.19 \\ -0.05 & 0.03 & 0.04 \\ -0.19 & 0.04 & 0.11 \end{bmatrix}
$$

$$
\begin{bmatrix} 0.94 & -0.08 & -0.79 \\ -0.08 & 0.10 & 0.05 \\ -0.79 & 0.05 & 0.84 \end{bmatrix}
\begin{bmatrix} 3.34 & -0.67 & -3.77 \\ -0.67 & 0.35 & 1.00 \\ -3.77 & 1.00 & 4.96 \end{bmatrix}
\begin{bmatrix} 1.51 & -0.08 & -0.46 \\ -0.08 & 0.03 & 0.02 \\ -0.46 & 0.02 & 0.15 \end{bmatrix}
\begin{bmatrix} 107.9 & -0.15 & -2.75 \\ -0.15 & 0.01 & 0.00 \\ -2.75 & 0.00 & 0.07 \end{bmatrix}
\begin{bmatrix} 0.38 & -0.02 & -0.16 \\ -0.02 & 0.03 & 0.01 \\ -0.16 & 0.01 & 0.08 \end{bmatrix}
\begin{bmatrix} 0.72 & -0.05 & -0.31 \\ -0.05 & 0.03 & 0.02 \\ -0.31 & 0.02 & 0.15 \end{bmatrix}
$$

(a)

$$
\begin{bmatrix} 0.15 & -0.04 & -0.13 \\ -0.04 & 0.03 & 0.05 \\ -0.13 & 0.05 & 0.15 \end{bmatrix}
\begin{bmatrix} 1.15 & 0.02 & -0.22 \\ 0.02 & 0.02 & -0.01 \\ -0.22 & -0.01 & 0.05 \end{bmatrix}
\begin{bmatrix} 1.56 & -0.23 & -1.47 \\ -0.23 & 0.16 & 0.32 \\ -1.47 & 0.32 & 1.80 \end{bmatrix}
$$

$$
\begin{bmatrix} 1.50 & -0.06 & -0.27 \\ -0.06 & 0.01 & 0.01 \\ -0.27 & 0.01 & 0.05 \end{bmatrix}
\begin{bmatrix} 8.19 & 0.05 & -0.49 \\ 0.05 & 0.02 & -0.01 \\ -0.49 & -0.01 & 0.03 \end{bmatrix}
\begin{bmatrix} 0.75 & -0.06 & -0.26 \\ -0.06 & 0.03 & 0.02 \\ -0.26 & 0.02 & 0.10 \end{bmatrix}
\begin{bmatrix} 0.34 & -0.03 & -0.15 \\ -0.03 & 0.03 & 0.01 \\ -0.15 & 0.01 & 0.08 \end{bmatrix}
\begin{bmatrix} 1.04 & -0.12 & -0.29 \\ -0.12 & 0.06 & 0.04 \\ -0.29 & 0.04 & 0.09 \end{bmatrix}
\begin{bmatrix} 4.31 & 0.04 & -0.59 \\ 0.04 & 0.04 & -0.01 \\ -0.59 & -0.01 & 0.09 \end{bmatrix}
\begin{bmatrix} 0.22 & -0.01 & -0.15 \\ -0.01 & 0.02 & 0.01 \\ -0.15 & 0.01 & 0.13 \end{bmatrix}
\begin{bmatrix} 0.46 & -0.02 & -0.21 \\ -0.02 & 0.02 & 0.01 \\ -0.21 & 0.01 & 0.11 \end{bmatrix}
$$

$$
\begin{bmatrix} 0.98 & -0.05 & -0.16 \\ -0.05 & 0.01 & 0.01 \\ -0.16 & 0.01 & 0.03 \end{bmatrix}
\begin{bmatrix} 4.97 & -0.05 & -0.37 \\ -0.05 & 0.01 & 0.00 \\ -0.37 & 0.00 & 0.03 \end{bmatrix}
\begin{bmatrix} 1.79 & -0.03 & -0.22 \\ -0.03 & 0.01 & 0.00 \\ -0.22 & 0.00 & 0.03 \end{bmatrix}
\begin{bmatrix} 0.81 & -0.02 & -0.28 \\ -0.02 & 0.03 & 0.00 \\ -0.28 & 0.00 & 0.11 \end{bmatrix}
\begin{bmatrix} 49.2 & -0.19 & -1.63 \\ -0.19 & 0.02 & 0.00 \\ -1.63 & 0.00 & 0.05 \end{bmatrix}
\begin{bmatrix} 0.48 & -0.04 & -0.19 \\ -0.04 & 0.02 & 0.01 \\ -0.19 & 0.01 & 0.08 \end{bmatrix}
\begin{bmatrix} 4.43 & -0.11 & -0.57 \\ -0.11 & 0.02 & 0.01 \\ -0.57 & 0.01 & 0.08 \end{bmatrix}
\begin{bmatrix} 9.85 & -0.25 & -2.32 \\ -0.25 & 0.03 & 0.06 \\ -2.32 & 0.06 & 0.56 \end{bmatrix}
$$

$$
\begin{bmatrix} 4.31 & 0.01 & -1.11 \\ 0.01 & 0.05 & -0.02 \\ -1.11 & -0.02 & 0.31 \end{bmatrix}
\begin{bmatrix} 0.50 & -0.03 & -0.18 \\ -0.03 & 0.01 & 0.01 \\ -0.18 & 0.01 & 0.08 \end{bmatrix}
\begin{bmatrix} 0.53 & 0.00 & -0.16 \\ 0.00 & 0.02 & -0.01 \\ -0.16 & -0.01 & 0.05 \end{bmatrix}
\begin{bmatrix} 3.31 & -0.26 & -1.28 \\ -0.26 & 0.05 & 0.11 \\ -1.28 & 0.11 & 0.52 \end{bmatrix}
\begin{bmatrix} 2.29 & 0.00 & -0.52 \\ 0.00 & 0.03 & -0.01 \\ -0.52 & -0.01 & 0.13 \end{bmatrix}
\begin{bmatrix} \\ \\ \\ \end{bmatrix}
\begin{bmatrix} 1.75 & -0.08 & -2.19 \\ -0.08 & 0.05 & 0.08 \\ -2.19 & 0.08 & 3.02 \end{bmatrix}
\begin{bmatrix} 172.5 & 0.42 & -6.02 \\ 0.42 & 0.07 & -0.02 \\ -6.02 & -0.02 & 0.21 \end{bmatrix}
$$

(b)

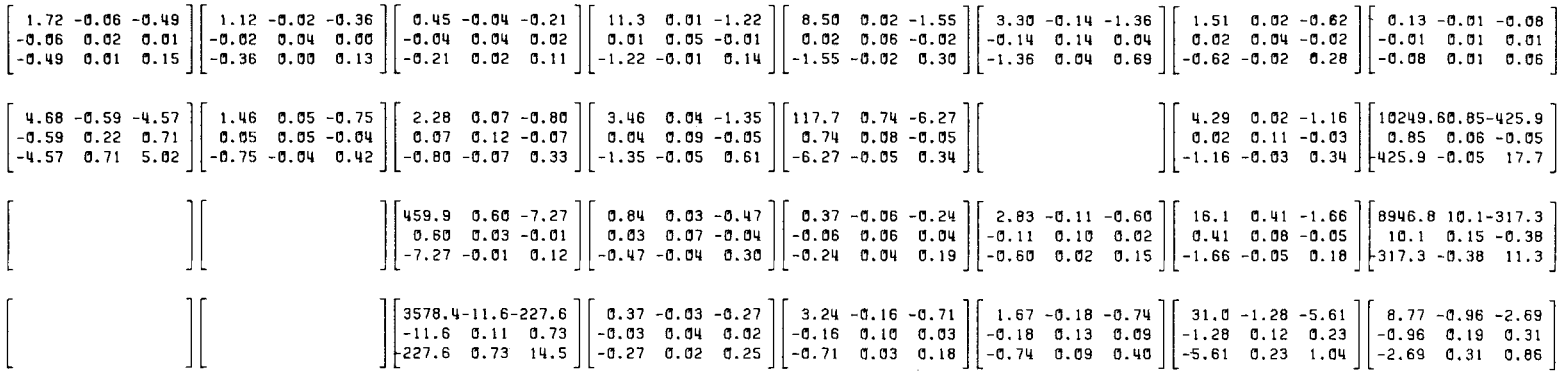

(c)

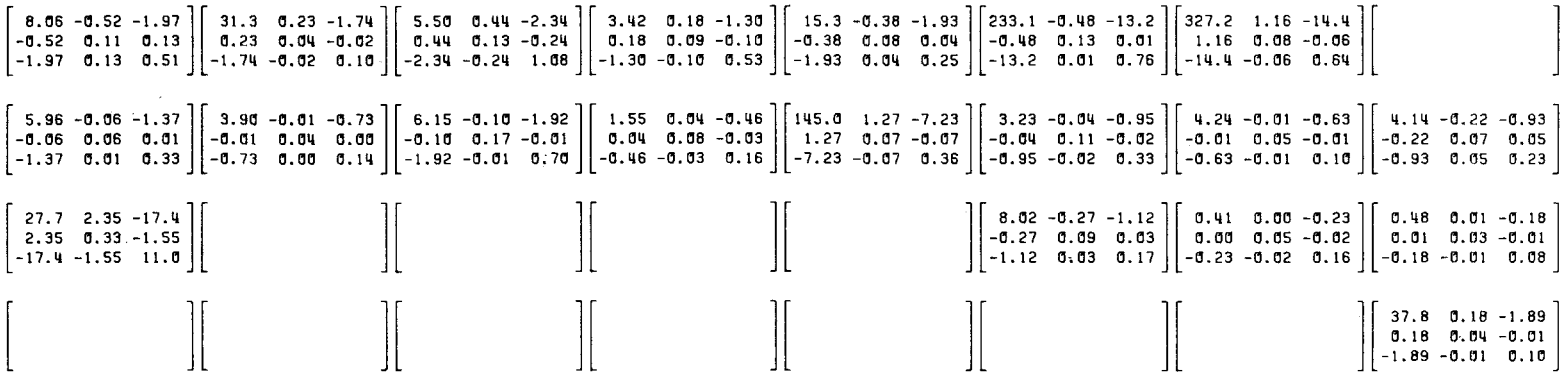

(d)

Figure 4. Each pair of brackets contains the covariance or error matrix ϵ for the Gumbel III parameters of a single 4° cell. For ease of reference the matrices are organized so that the top left matrix corresponds to the north-west corner or cell 01 of a region, and all the rest are relatively arranged to match both their geographic positions shown in Fig. 1, and individual cell diagrams shown in Fig. 3. Matrix elements of ϵ are

$$\begin{pmatrix} \sigma_w^2 & \sigma_{uw}^2 & \sigma_{\lambda w}^2 \\ \sigma_{wu}^2 & \sigma_u^2 & \sigma_{\lambda u}^2 \\ \sigma_{w\lambda}^2 & \sigma_{u\lambda}^2 & \sigma_\lambda^2 \end{pmatrix}$$

where the matrix diagonal gives the cell parameter variances in the order $\sigma_w^2, \sigma_u^2, \sigma_\lambda^2$: (a) ϵ matrices for the 4° cells of Region 1; (b) ϵ matrices for the 4° cells of Region 2; (c) ϵ matrices for the 4° cells of Region 3; (d) ϵ matrices for the 4° cells of Region 4.

represent the 'probable' largest earthquake of the next 75-yr, providing that NPER is sufficiently small compared to the 75-yr prediction length.

Yegulalp (1974) has calculated confidence bounds on the most probable largest magnitude (mode) of the next T years, using annual extremes, and his upper bound to $m_1(T)$ at the probability level α is

$$m_1^{\alpha} \approx w - (w - u)\,[-1/T \cdot \ln(1 - \alpha/2)]^{\lambda}. \tag{31}$$

It is important to know the confidence bound on any prediction but this method suffers from two practical disadvantages. The upper uncertainty interval, given by $\delta\alpha = m_1^{\alpha} - m_1$ depends on $T^{-\lambda}$, and so for large T the value of $\delta\alpha$ is very small, tending to zero as the prediction length increases. Secondly, m_1^{α}, like m, is upper bounded at the limiting magnitude value w. These two related properties of equation (31) are most undesirable in the present application in view of the large uncertainties σ_w estimated with each upper limit w. In practice it is desirable that the upper bound on a prediction should be allowed to transcend what is really an uncertain value for the upper magnitude limit w. A preferable and more realistic value of the prediction uncertainty estimate σ_m can be obtained from:

$$\sigma_m^2 \approx \sigma_w^2 \left(\frac{\partial m}{\partial w}\right)^2 + \sigma_\lambda^2 \left(\frac{\partial m}{\partial \lambda}\right)^2 + \sigma_u^2 \left(\frac{\partial m}{\partial u}\right)^2 + 2\sigma_{w\lambda}^2 \left(\frac{\partial m}{\partial w}\right)\left(\frac{\partial m}{\partial \lambda}\right) \ldots \tag{32}$$

where the actual prediction $m(T)$ may be the modal, median, mean value of equations (28), (29) and (30), or the return period estimate $m_4(75)$ predicted by rearranging equation (9). Partial derivatives in equation (32) are derived from the equation giving the particular statistic chosen to predict $m(T)$. Table 3 gives the 75-yr earthquake predicted for each cell of Region 1. This table gives the most likely, modal, earthquake of the next 75 yr, and the

Table 3. 75-yr earthquake magnitudes $m(75)$ predicted for each cell of Region 1. The modal value m_1 and the return period estimate m_4 are listed for 75 yr, along with standard deviations σ_m estimated using (a) Yegulalp's (1974) upper bound uncertainty formula for $\delta\alpha = \sigma_m$, (b) diagonal elements of the matrix ϵ, (c) all elements of the matrix ϵ. Cells of Region 1 and 2 which overlap by three quarters of their area are indicated.

Cell		$m_1(75)$	σ_{m_1} (a)	σ_{m_1} (b)	σ_{m_1} (c)	$m_4(75)$	σ_{m_4} (b)	σ_{m_4} (c)	Overlap
1.01	44, 4	6.05	0.02	0.44	0.32	5.97	0.43	0.28	
1.02	44, 8	5.54	0.01	0.33	0.28	5.49	0.32	0.25	
1.03	44,12	5.69	0.02	0.35	0.27	5.64	0.34	0.25	
1.04	44,16	6.13	0.25	0.87	0.21	6.03	0.81	0.21	
1.05	44,20	6.22	0.01	0.59	0.46	6.12	0.58	0.40	2.01
1.06	44,24	6.93	0.25	1.81	0.45	6.83	1.69	0.45	2.02
1.09	40, 4	6.43	0.08	2.23	1.28	6.31	2.13	1.16	
1.10	40, 8	5.62	0.00	0.41	0.33	5.53	0.40	0.28	
1.11	40,12	6.18	0.09	0.56	0.29	6.09	0.53	0.27	
1.12	40,16	6.32	0.16	1.02	0.34	6.25	0.96	0.33	
1.13	40,20	6.57	0.12	0.76	0.36	6.48	0.72	0.34	2.09
1.14	40,24	7.10	0.11	1.09	0.58	6.97	1.04	0.53	2.10
1.15	40,28	7.15	0.20	0.75	0.31	6.99	0.70	0.29	2.11
1.16	40,32	7.19	0.01	0.65	0.50	7.07	0.64	0.43	2.12
1.17	36, 4	6.50	0.42	6.71	0.93	6.43	6.36	1.00	
1.18	36, 8	5.66	0.35	15.04	1.04	5.62	14.40	1.22	
1.19	36,12	6.96	0.42	1.53	0.36	6.82	1.44	0.36	
1.20	36,16	6.17	0.29	1.82	0.36	6.08	1.70	0.37	
1.21	36,20	7.54	0.24	0.93	0.30	7.44	0.87	0.30	2.17
1.22	36,24	7.70	0.84	3.97	0.27	7.62	3.81	0.30	2.18
1.23	36,28	6.95	0.10	0.66	0.31	6.83	0.63	0.28	2.19
1.24	36,32	6.34	0.02	0.62	0.46	6.26	0.59	0.41	2.20
1.25	32, 4	6.14	0.00	0.97	0.86	6.08	0.96	0.74	
1.27	32,12	5.64	0.00	1.82	1.55	5.61	1.77	1.36	
1.29	32,20	6.78	0.11	1.18	0.54	6.69	1.12	0.50	2.25
1.30	32,24	7.23	0.62	5.21	0.39	7.17	4.99	0.45	2.26
1.31	32,28	7.11	0.02	0.62	0.45	6.99	0.61	0.39	2.27
1.32	32,32	6.50	0.03	0.85	0.59	6.39	0.82	0.51	2.28

75-yr return period earthquake. The upper bound uncertainty at one standard deviation from this modal value is tabulated according to equation (31), and standard deviations using equation (32) are calculated both with and without the off-diagonal terms of the covariance matrix. It is obvious from this table that the upper bound interval $\delta\alpha$ is often unacceptably small, only assuming a reasonable value when the 75-yr earthquake in a cell is considerably smaller than w.

The values of σ_m, on both the modal and return period estimates of $m(75)$, are calculated first using only the diagonal terms of the error matrix. These values of σ_m are much more realistic than the values of $\delta\alpha$, however, the final improvement comes when the off-diagonal terms of ϵ are incorporated into estimates of σ_m. Cell 1.09 illustrates these last points. The upper limit to magnitude is about 6.63 ± 2.25. λ is also quite uncertain being about 0.56 ± 0.7, but u is quite well determined being 4.13 ± 0.27. Given these parameters, a value of $\delta\alpha = 0.08$ is clearly optimistic, whereas σ_m around 2.2, obtained using diagonal terms of ϵ, appears more reasonable. The use of off-diagonal terms exploiting the negative covariance $\sigma^2_{w\lambda}$ improves the estimate of σ_m, giving a value of $\sigma_m = 1.2$.

The 75-yr return period earthquake and σ_m in each cell of the three other major regions are listed in Table 4. Standard deviations σ_m on $m_4(75)$ for the cells of Region 4 are generally the largest and this confirms the view that the data for Region 4 are the more unreliable of the data sets which are analysed in this study. On the other hand estimates of σ_m for the other three regions are usually less than 0.5.

8 Contour maps of seismic risk

Dividing the seismicity data into 4° geographic cells readily lends itself to mapping of the results to represent regional differences in seismic risk. Values of $m_4(75)$, listed in Tables 3 and 4, are mapped and contoured in Figs 5 and 6 (Maps 1 and 2).

8.1 GENERAL CONSIDERATIONS

Maps of seismic risk should in some way describe the probability of occurrence of earthquakes of different sizes in different regions. The production of maps of a or b in equation

Table 4. 75-yr earthquake magnitudes $m_4(75)$ predicted for each cell of Regions 2, 3 and 4 with σ_m estimated using all elements of ϵ.

Region 2				Region 3				Region 4			
Cell		$m_4(75)$	σ_m	Cell		$m_4(75)$	σ_m	Cell		$m_4(75)$	σ_m
2.01	44,19	5.56	0.27	3.01	35,42	5.70	0.19	4.01	32,65	7.50	1.18
2.02	44,23	6.33	0.21	3.02	35,46	5.82	0.19	4.02	32,69	7.73	0.61
2.03	44,27	5.96	0.86	3.03	35,50	6.48	0.19	4.03	32,73	7.11	0.96
2.09	40,19	6.20	0.20	3.04	35,54	6.36	0.26	4.04	32,77	6.59	0.59
2.10	40,23	6.84	0.25	3.05	35,58	5.93	0.28	4.05	32,81	7.35	0.96
2.11	40,27	6.84	0.40	3.06	35,62	6.39	0.54	4.06	32,85	7.42	1.68
2.12	40,31	7.03	0.32	3.07	35,66	6.48	0.24	4.07	32,89	6.90	1.02
2.13	40,35	7.25	0.46	3.08	35,70	7.11	0.11	4.09	28,65	7.39	0.76
2.14	40,39	6.78	0.33	3.09	31,42	5.43	0.53	4.10	28,69	6.36	0.38
2.15	40,43	5.91	0.23	3.10	31,46	6.11	0.21	4.11	28,73	6.80	1.32
2.16	40,47	6.25	0.22	3.11	31,50	6.25	0.33	4.12	28,77	7.47	0.55
2.17	36,19	7.07	0.20	3.12	31,54	5.95	0.36	4.13	28,81	6.35	0.60
2.18	36,23	7.23	0.23	3.13	31,58	6.41	0.30	4.14	28,85	6.86	0.94
2.19	36,27	7.01	0.20	3.15	31,66	6.52	0.32	4.15	28,89	7.70	0.57
2.20	36,31	6.22	0.34	3.16	31,70	5.13	0.28	4.16	28,93	7.77	0.85
2.21	36,35	6.94	0.31	3.19	27,50	5.75	0.18	4.17	24,65	6.30	2.43
2.22	36,39	6.82	0.23	3.20	27,54	6.58	0.22	4.22	24,85	7.47	0.97
2.23	36,43	6.46	0.31	3.21	27,58	6.39	0.22	4.23	24,89	7.14	0.42
2.24	36,47	5.96	0.58	3.22	27,62	7.27	0.36	4.24	24,93	7.68	0.30
2.25	32,19	6.54	0.52	3.23	27,66	6.20	0.28	4.32	20,93	8.02	0.63
2.26	32,23	6.65	0.24	3.24	27,70	5.53	0.70				
2.27	32,27	6.54	0.22	3.27	23,50	5.58	0.39				
2.28	32,31	6.58	0.73	3.28	23,54	5.57	0.20				
2.29	32,35	5.55	0.31	3.29	23,58	6.97	0.39				
2.31	32,43	5.64	0.55	3.30	23,62	7.25	0.40				
2.32	32,47	7.69	0.58	3.31	23,66	5.73	0.32				
				3.32	23,70	6.00	0.35				

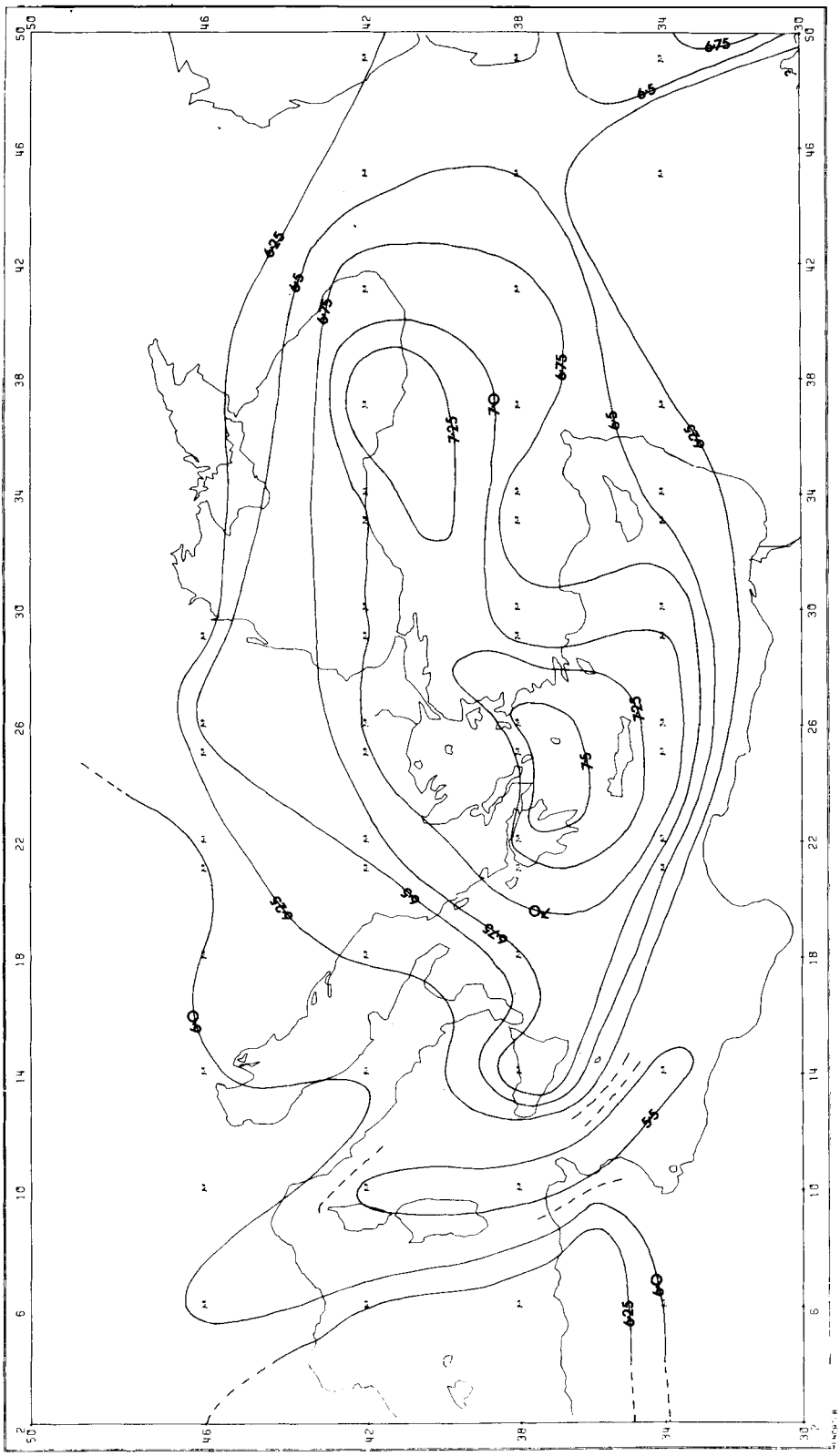

Figure 5. (Map 1) The Mediterranean through to the Caspian Sea. Values of the largest earthquake magnitude expected over an interval of 75 yr are forecast using $m_4(75)$ obtained from each 4° cell and the forecasts are contoured in one quarter magnitude intervals. The data contoured here is for the geographic Regions 1 and 2 and complete details of the individual cell forecasts of $m_4(75) \pm \sigma_{m_4}$ may be found in Tables 3 and 4. Several of the geographically central (mid-longitudes) values of $m_4(75)$ from which the contours of this map are constructed are obtained from cells which have three quarters of their area in common; this serves to check statistical stability of the map.

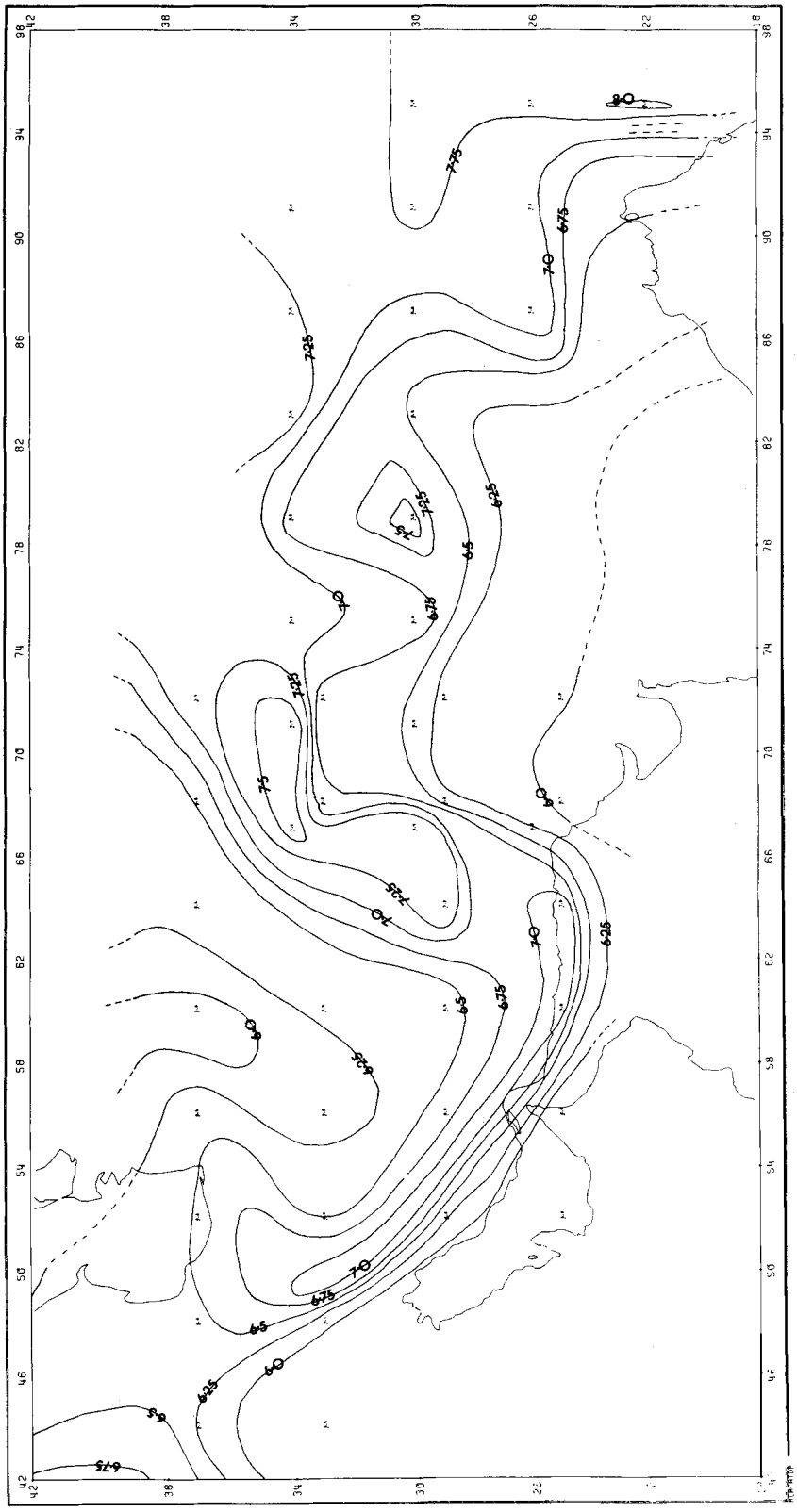

Figure 6. (Map 2) The Zagros mountains through to the Himalayas. The format of this map is similar to that described for Map 1 in Fig. 5. The data contoured is for the geographic Regions 3 and 4 and values of $m_4(75) \pm \sigma m_4$ for individual cells may be found in Table 4.

(1) was computed by several workers. However, a and b are parameters of a distribution, and it is necessary to extend these parameters to a combined seismological and probabilistic statement, for example a/b is the largest annual earthquake. With the results obtained in this paper it is possible to produce maps of the three parameters w, u and λ, and for both w and u these could certainly be interpreted probabilistically. However, mapping the distribution parameters moves away from simpler statements of seismic risk, such as how big the earthquakes in a region are, and how often they occur. Kaila & Rao (1975) map the return period T years for earthquakes of magnitude 6 or over. Essentially this shows the function $T(m)$ with the independent variable m fixed at 6 and $T(m)|_6$ contoured for a discrete set of T values. Alternatively we may consider $m(T)$, choose a standard value of T_0 years and contour $m(T)|_{T_0}$ at discrete m. Surprisingly, which route is taken need not be a trivial decision. Gumbel III has curvature convex with respect to an asymptotic upper magnitude limit, which implies that the gradients are of the form

$$\left.\frac{dm}{dT}\right|_{T\to\infty} \longrightarrow 0,$$

and

$$\left.\frac{dT}{dm}\right|_{m\to w} \longrightarrow \infty.$$

For large values of T or m perturbations to T make little difference to the predicted value of m, whereas perturbations to m can produce apparently drastic changes in T. The stable estimate of seismic risk using Gumbel III is given by estimating m at a given T, and stability is achieved through examining discrete levels of $m(T)|_{T_0}$. This approach is also in keeping with the philosophy of allowing $m(75) + \sigma_m$ to exceed the calculated upper limit to magnitude w, rather than using an uncertain estimate of w to constrain the uncertainties σ_m. It would now have been unrealistic if rapidly varying and unreliable values of return period (Knopoff & Kagan 1977) occurring in the region where w is uncertain and subject to $dT/dm \to \infty$, were accepted as reliable discriminators between regions of high and low seismic risk.

Seventy-five years is superficially the time extent of data in each cell, but in practise the time span is usually less than this and a small degree of extrapolation is required. In many instances $m_4(75) + \sigma_m$ does equal or exceed w, but it is preferable to imply that $m_4(75) + 2\sigma_m$, is about the 98 per cent confidence level (2 per cent chance of being exceeded) for the earthquake magnitude with mean interval of occurrence of about 75 yr, rather than imply that the return period for this magnitude of earthquake is somewhere near to an infinite span of years.

8.2 SOUTHERN EUROPE THROUGH TO EASTERN TURKEY AND THE CASPIAN SEA

When preliminary results were first obtained for Region 1 an attempt was made to produce a totally objective contour map of $m_4(75)$ entirely by computer (Burton 1978b). This approach has been abandoned for the moment because it is difficult to produce an algorithm which contours successfully at the boundaries of regions or where data is sparse. Nevertheless the contours of Maps 1 and 2 have been drawn as objectively as seemed reasonable. The seismicity of the western area of Map 1 will be discussed first.

8.2.1 North Africa and western Mediterranean regions

In northern Italy the Friuli earthquake of 1976 May 6 has a magnitude of about 6.2 (reported by the European Mediterranean Seismological Centre 1976), and the activity around Friuli is not unreasonably represented by the magnitude 6 contour line (for $m_4(75)$) which runs through these northwestern cells of Map 1. Franke & Gutdeutsch (1974) investigated the seismicity within Austria listing 72 earthquakes for the period 1905 to 1973 with a largest magnitude of 5.3 with epicentre around 48° N, 16° E. This epicentre is north-east of Friuli in keeping with the positioning of the magnitude 6 contour, and the general downward gradient of seismicity trending north-westwards in this region of Europe. Ahorner & Rosenhauer (1975) have studied the northern Rhine area of central Europe extending south as far as about 49° N with data for the period 1750 to 1970. By extrapolation Ahorner & Rosenhauer estimate the maximum magnitude for the region to be about 6.25 and in the most seismically active region, the western part of the Lower Rhine Graben, their results suggest that $m_4(75)$ is approximately just over 6. This is not inconsistent with the general picture of seismicity derived for the relatively low and uncertain levels of seismicity in the north-west of Map 1.

To the west the data are again sparse but outside the western bound of the map there is well established seismic activity in south-east Spain, zoned as early as 1927 by Pastor (1927) who shows earthquakes in the western Mediterranean and through into the Straits of Gibraltar. Several earthquakes are also known to have occurred within the vicinity of Gerona and Barcelona in northeastern Spain, and this gradient of increased seismicity in the western Mediterranean is in accord with the higher activity illustrated by the 6¼ contour running through the westernmost cells.

Further anticlockwise are the Atlas Mountains and Algeria and Tunisia in North Africa. One earthquake of note is the Orleansville earthquake of 1954 (Heezen & Ewing 1955), which had a magnitude around 6.7 and caused both underground pipes and submarine cables to be broken. This occurred near the high activity about 3° W of the edge of the map towards the Straits of Gibraltar, but eastwards, along the Atlas Mountains and the coastal regions of North Africa, several earthquakes of magnitude 5 and 6 are detailed by Gorshkov (1961), although the elliptical contour enclosing the low of seismicity from Corsica, through Sardinia and extending south-eastwards, does not seem to have been described in the available literature. The African boundary to Map 1 shows little seismic activity elsewhere until the Red Sea is reached, and this activity seems to be highly localized despite the number of epicentres increasing southwards towards the junction of the Red Sea and the Gulf of Aden (Fairhead & Girdler 1971). Gouin (1976) finds evidence of magnitude 6 events within the Ethiopian land mass. Most of these earthquakes are remote from the south of the map and there is very little evidence of seismic activity elsewhere in Libya and Egypt.

8.2.2 Vrancea, in Romania, and Yugoslavia

Moving north to the Vrancea earthquakes, Enescu, Marza & Zamarca (1974) have applied Gumbel I to data for the period 1934–73 and so obtained an equation which implies that $m_4(75)$ is about 7.2. The present results for the 4° cell which includes Vrancea (cell 1.06) give $m_4(75)$ as 6.8 ± 0.45 and the characteristic magnitude u obtained for 2 yr extremes is 4.98 ± 0.17 whereas Enescu *et al.* show a magnitude just over 5, with a return period of about 2 yr. The agreement is excellent and the deflection of the 6¼ and 6½ contours to the north of Vrancea is well founded. The 6¼ and 6½ contours show a trend south-westwards into Yugoslavia and Nedeljkovic (1950) has presented a macroseismic map for the intensities generated by shallow earthquakes consistent with the occasional magnitude over 6.

8.2.3 Italy and Calabria

The Appennine structure of central Italy does not stand out in this analysis, but the earthquakes of the Tyrrhenian Sea are very clear giving a westward extension to the general east–west trend of seismicity. Most of the earthquakes of the Tyrrhenian Sea, Sicily and the western seaboard of Calabria are contained by cell 1.19 and the 75-yr earthquake is $m_4(75) = 6.8$ in keeping with Caputo *et al.*'s (1974) region S. Caputo *et al.* show higher activity in central Italy than in Sicily and its northern seaboard, although this does not seem supported by this work or the history of great earthquakes (Davison 1936). Cell 1.11 containing the data for central Italy reveals a high level of seismic activity similar to Richter's (1958) description but mostly around magnitude 5, magnitudes around 6 being unusual as indicated by a value of 6.1 for $m_4(75)$ and 6.4 ± 0.6 for w. The activity associated with central Italy does not seem to reach the higher magnitudes associated with Sicily and the Tyrrhenian.

Carefully performed fault plane solutions (Ritsema 1967) give an insight into the tectonics of a region and Riuscetti & Schick (1975) conclude that many shallow earthquakes are of strike-slip character, with a probable east–west strike, in agreement with McKenzie (1972). The Messina earthquake of 1908 is exceptional to this pattern and surveys subsequent to this event describe general changes in level which are consistent with normal faulting (Davison 1936), and the fault plane solution of Riuscetti & Schick confirms this. Fault plane solutions of Cagnetti, Pasquale & Polinari (1978) also give fairly good agreement with this regional pattern. One interpretation is that there is a general eastward movement of the region with exceptional normal faulting along the old pre-Calabrian Comiso line into the Appenines, and strike-slip faulting occurring on the more recent faults in an east–west direction. This is consistent with the westward bulge of seismicity shown in Map 1 around Sicily, but it poses the question whether this pattern should be continued further westwards to make the obvious junction with the contours associated with the Atlas mountains in North Africa. The data do not allow this extension but indicate a relative low of seismicity between North Africa and Sicily, indicated on the map by a regional low which is also associated with Corsica and Sardinia. The western boundary to the Appennine area is indicated by a dashed contour because of uncertainty where this contour should be traced when taken in conjunction with Sicily and North Africa.

8.2.4 Greece

The contours of Map 1 associated with the high seismicity of Greece, the sea of Crete and the Anatolian Fault are well defined by the available results.

Both qualitative and numerical results of Galanopoulos (1968, 1971) are in accord with Map 1 for Greece showing the highest seismicity in the east in conjunction with the northern extent of the Sea of Crete. Galanopoulos (1971) indicates a magnitude of 7.3 for the 75-yr earthquake in mainland Greece, in excellent agreement with cell 1.21. Makropoulos (1978) has relocated the epicentres of many earthquakes ($M_s \geq 5.0$, 1912–63) of Greece, the Ionian Arc and Crete, finding that earthquakes in the arc south of Crete relocate from depths around 120 km to around 70 km. This implies a higher degree hazard associated with the local earthquake risk and a tendency, similarly observed by Riuscetti & Schick for the Tyrrhenian, for the elimination of supposedly intermediate depth earthquakes in the Mediterranean.

8.2.5 Turkey

The North Anatolian Fault generates a local high of seismicity with $m_4(75) = 7.25$ confined within an east–west direction. It is tempting to join the 7.25 contour circling the Ionian

Arc, Crete and western Turkey to the high on the North Anatolian Fault in northeastern Turkey, but these two highs do seem to be distinct and separate. An explanation may be invoked from Crampin & Uçer (1975), who suggest that the western Anatolian Fault splits into three near to Adapazari, not too remote from Bursa, which Ambraseys (1970) suggests is the western end of the Anatolian fault rather than a region where the fault is subdivided. The deep water in the Marmara Sea, the volcanoes in Bulgaria and the intermediate depth earthquakes of Romania may indicate a fossil subduction zone. Ambraseys & Zatopek (1969) have observed an apparent migration of seismicity from east to west along the North Anatolian and so this high of seismicity may not be absolutely stable. Ambraseys (1971) also describes historical seismicity of Istanbul which appears time variant, but this required 2000 yr of data and is unlikely to be significant in the time span analysed here.

Kaila & Narain (1971) and Kaila & Rao (1975) have produced contour maps of return periods for earthquakes of magnitude 6 and like Map 1 they show that east of Athens the main north-west to south-east trend of the Balkan region takes a right angle bend towards Ankara, and this then appears to be a south-west to north-east trending extension of the Balkan seismic zone extending to the southern margin of the Black Sea. The trend in the contours around Sicily and the bend in seismicity in the Sea of Crete are very distinct features in Map 1. A distinction between these results and those of Kaila & Rao, besides the method, is that some large differences in detail seem to arise because Kaila & Rao do not appear to allow for as wide a range of seismic activity in Europe.

8.3 IRAN THROUGH TO INDIA

Results for the third and fourth major regions are contoured in Fig. 6 (Map 2). There is a major difference between these two maps. The geographical region of Map 1 is largely surrounded by regions of lower seismicity whereas Map 2 is bounded to the north, east and south-east by regions of similar seismicity and consequently several of the contours of Map 2 are necessarily left open at the edges of the map. (The north-west of Map 2 and the south-east of Map 1 overlap which aids contouring and continuity between Maps 1 and 2.)

8.3.1 Zagros and Elburz Mountains

The seismicity of the Zagros Mountains of Iran, is depicted similarly to Kaila, Rao & Narain (1974) by a steep-sided ridge, and the long documentation (e.g. Wilson 1930) suggests a local extension of the obvious Zagros ridge of seismicity along the Elburz range, although this particular contour is clearly subject to an uncertainty compounded by rogue earthquakes such as Dasht-e-Bayaz (13/8/1978, $M_S = 7.3$, Bayer, Heuckroth & Karim 1969), occurring close to a magnitude 6 contour of $m_4(75)$ in central Iran. However, North (1977) and McKenzie (1972) point out that the Dasht-e-Bayaz earthquake with large left-lateral strike-slip substantiated by Ambraseys & Tchalenko (1969), is difficult to explain in terms of regional plate motions, whereas elsewhere in northern Iran sparce seismicity is usually characterized by thrust mechanisms (Ambraseys 1963). McKenzie (1972) interprets the Zagros seismicity as a boundary between the Iranian and Arabian plates, the Elburz mountains separating the Iranian and South Caspian plates. North (1974) attempts to reconcile seismic slip rates with slip rates predicted from a plate tectonic model of the region and finds that the former are much the smaller. The implication is that creep is a major contribution to deformation which unfortunately prevents the simple correlation of Map 1 or Map 2 with slip phenomena at plate boundaries.

8.3.2 Makran Ranges

The elbow between the dominant trends of the Zagros Mountains and the Baluchistan Arc seems to occur slightly north of the Makran Coast Ranges, towards the Central Makran Range. Some earthquakes do occur in the Makran west of Baluchistan (Pendse 1948) but seismicity data is sparse, leaving two separate highs associated with the Zagros Mountains and the Baluchistan Arc within the $m_4(75) = 6.75$ contour of the overall reginal trend. The sharp elbow in the Makran might have been expected to show seismic properties similar to the two major syntaxial bends of the Himalayas, whereas a relative seismic low is observed. The higher seismicity of the Himalayan complex, compared to the Zagros mountains leads to North's (1974) and Chen & Molnar's (1977) interpretation that the major contribution to the slip rate in the Himalayas is seismic, whereas in Iran fault creep is significant. The implication from this map is that a large degree of creep most probably takes place in the relatively seismically quiet syntaxial bend in the Makran, absorbing a complex combination of both rotational and compressional strain energy associated with the northwards motion of the Indian plate.

8.3.3 Baluchistan, Himalayan and Burmese Arcs

The Indian subcontinent is bordered by three convex mountain arcs, the Burmese arc to the east, Himalayan arc in the north and the Baluchistan arc in the west: the supposedly passive Indian Peninsular underthrusts into these arcs (Chouhan 1970a, b) accounting for most of the observed seismicity (Kaila, Gaur & Narain 1972) of these regions in Map. 2. The east and west ends of the Himalayan arc form syntaxial bends at Assam and Kashmir, which are even more seismically active than the rest of the chain. Hindukush and Pamir knot earthquakes stand out as a conspicuous high of seismicity with $m_4(75)$ around 7.75, which is in keeping with the local studies of Chouhan (1966), Gaur & Chouhan (1968) and Chouhan & Srivastava (1973), and fault plane solutions of Armbruster, Seeber & Jacob (1978) show strike-slip or reverse faulting compatible with the underthrusting of Eurasia by the Indian plate. South of the Hindukush, in the Punjab, a square plateau of seismicity is contoured abutting the steep gradient leading to the Hindukush, and compatible with the increase of strain energy prior to its main release in the Hindukush. Eastwards, a local high of seismicity is correlated with the Kumaon Mountains east of Delhi, within which the dominant seismic trend (Chouhan 1975) is north-west to south-east. Earthquakes of Assam (Chouhan, Gaur & Mithal 1966) are not clearly depicted as a local high because the major trend in the south-east of Map 2 is a continuation outside the map into the Andeman Islands along the Sunda Arc. Fault plane solutions (Chouhan & Srivastava 1977; Chen & Molnar 1977) indicate a transition from the Himalayan Frontal Thrust to strike-slip faulting extending south towards the Sunda Arc. The $m_4(75) = 7.25$ contour to the north-east (cells 4.05, 4.06) constituted a boundary problem, and its position indicating a south-west to north-east trend in seismicity outside the map remains conjectural until the evidence of Molnar & Tapponnier (1975) is included to show the Altyn Tagh fault on Earth Resources Technology Satellite photographs striking prominently south-west to north-east in this region.

9 Conclusions

It is axiomatic that any seismic risk analysis must include an error analysis if it is to demonstrate some degree of validity. Even with such careful considerations we should not expect

to obtain a complete statistical description of seismicity, and presumably the present analysis is itself influenced by inhomogeneity in the data. This is a problem which can only be resolved with the passage of time. However, when extreme value statistics are used it is possible to choose appropriate plotting points, to weight the individual extreme values and to select extreme intervals in accord with the available data. This paper has demonstrated how Gumbel III may then be effectively fitted to seismicity data, and in particular to seismicity data which is divided in a cellular manner rather than division by inclusion of tectonic considerations.

An evaluation of the covariance matrix among the three parameters of Gumbel III demonstrates that the characteristic value u is usually well determined with small uncertainty, whereas both the parameters of curvature and the upper bound to magnitude often show large uncertainties. Clearly, it is not appropriate to extract isolated parameters from a distribution as a complete description of seismic risk, and upper limits to the magnitude of earthquakes in a region should only be considered along with a knowledge of associated uncertainty.

Some examples of seismicity show exceptionally large or uncertain values for w. In these cases the implication is that the phenomenon of curvature is either not yet established from the regional seismicity, or that a simpler, two parameter distribution would give an adequate statistical description of the seismicity. Usually a degree of curvature is established which implies an asymptotic approach to the upper bound to earthquake magnitude, rather than a linear approach terminated by a dramatic truncation at the value of the upper bound to magnitude.

Gumbel III has one independent parameter: u. A large negative covariance exists between the other two parameters: w and λ. This negative covariance has two implications. It significantly improves the forecasting of return periods of large earthquakes. It implies that this distribution will usually be conservative in its approach to the upper magnitude bound from above.

Despite the fact that Gumbel III may be skew, the largest earthquake with a long return period, 75 yr, is independent of the distribution statistic chosen for its description. This leads to considerable simplification. The ensuing results for the 75-yr earthquake lend themselves to the production of regional seismic risk maps. The observation of curvature of the seismicity distribution implies that any such map which depicts magnitude for a given return period is intrinsically more stable than one which plots return periods for a given magnitude to be exceeded. The two seismic risk maps presented here cover the regions of southern Europe through to eastern Turkey and the Caspian Sea, and Iran through to India. Both of these maps show that the seismicity associated with the known seismotectonics is usually clearly delineated by the seismic risk, and an excellent agreement is found between the coherent picture provided by these maps and many local studies of seismicity within southern Europe, the Middle East and India.

Acknowledgments

I am grateful for useful discussions with A. W. B. Jacob, C. Makropoulos, G. Neilson and P. L. Willmore, to S. Crampin for his critique of the manuscript, and especially to R. W. McGonigle, particularly for his help with computing. This work was supported by the Natural Environment Research Council and is published with the approval of the Director of the Institute of Geological Sciences.

References

Ahorner, L. & Rosenhauer, W., 1975. Probability distribution of earthquake accelerations with applications to sites in the Northern Rhine area, Central Europe, *J. Geophys.*, **41**, 581–594.

Aki, K., 1965. Maximum likelihood estimate of b in the formula $\log N = a - bM$ and its confidence limits, *Bull. Earthq. Res. Inst., Tokyo Univ.*, **43**, 237–239.

Ambraseys, N. N., 1963. The Buyin-Zara (Iran) earthquake of September 1962: A field report, *Bull. seism. Soc. Am.*, **53**, 705–740.

Ambraseys, N. N., 1970. Some characteristic features of the Anatolian fault zone, *Tectonophysics*, **9**, 143–165.

Ambraseys, N. N., 1971. Value of historical records of earthquakes, *Nature*, **232**, 375–379.

Ambraseys, N. N. & Tchalenko, J. S., 1969. The Dasht-e-Bayaz (Iran) earthquake of 1968 August 31: A field report, *Bull. seism. Soc. Am.*, **59**, 1751–1792.

Ambraseys, N. N. & Zatopek, A., 1969. The Mudurnu Valley, West Anatolia, Turkey, earthquake of 1967 July 22, *Bull. seism. Soc. Am.*, **59**, 521–589.

Armbruster, J., Seeber, L. & Jacob, K. H., 1978. The northwestern termination of the Himalayan mountain front: active tectonics from microearthquakes, *J. geophys. Res.*, **83**, B1, 269–282.

Bayer, K. C., Heuckroth, L. E. & Karim, R. A., 1969. An investigation of the Dasht-e-Bayaz, Iran earthquake of August 31, 1968, *Bull. seism. Soc. Am.*, **59**, 1793–1822.

Burton, P. W., 1978a. Perceptible earthquakes in the United Kingdom, *Geophys. J. R. astr. Soc.*, **54**, 475–479.

Burton, P. W., 1978b. The application of extreme value statistics to seismic hazard assessment in the European area, *Proc. Symp. Anal. Seismicity and on Seismic Risk*, Liblice, 1977 October 17–22, pp. 323–334, Academia, Prague.

Burton, P. W., 1978c. The IGS file of seismic activity and its use for hazard assessment, *Inst. Geol. Sci., seism. Bull.* No. 6, HMSO.

Cagnetti, V., Pasquale, V. & Polinari, S., 1978. Fault plane solutions and stress regime in Italy and adjacent regions, *Tectonophysics*, **46**, 239–250.

Caputo, M., Keilis-Borok, V. I., Kronrod, T. L., Molchan, G. M., Panza, G. F., Piva, A., Podgaetskaja, V. M. & Postpischl, D., 1974. The estimation of seismic risk for central Italy, *Annali Geofis.*, **27**, 349–365.

Chen, W. & Molnar, P., 1977. Seismic moments of major earthquakes and the average rate of slip in central Asia, *J. geophys. Res.*, **82**, 2945–2969.

Chinnery, M. A. & North, R. G., 1975. The frequency of very large earthquakes, *Science*, **190**, 1197–1198.

Chouhan, R. K. S., 1966. Regional strain release characteristics for Indian regions, *Bull. seism. Soc. Am.*, **56**, 749–754.

Chouhan, R. K. S., 1970a. Earthquakes in the Himalayan region, *Pure appl. Geophys.*, **81**, 112–118.

Chouhan, R. K. S., 1970b. Seismotectonics of Hindukush, *Pure appl. Geophys.*, **82**, 108–118.

Chouhan, R. K. S., 1975. Seismotectonics of Delhi region, *Proc. Indian natn. Sci. Acad.*, **41**, A, 429–447.

Chouhan, R. K. S., Gaur, V. K. & Mithal, R. S., 1966. Seismicity of Assam, *Third Symposium on Earthquake Eng.*, University of Roorkee, India, 1966 November 4–6.

Chouhan, R. K. S. & Srivastava, V. K., 1973. Statistics of Indian earthquakes – frequency energy distribution, *Annali Geofis.*, 27, 59–68.

Chouhan, R. K. S. & Srivastava, V. K., 1975. Focal mechanisms in northeastern India and their tectonic implications, *Pure appl. Geophys.*, **113**, 467–482.

Crampin, S., Fyfe, C. J., Bickmore, D. P. & Linton, R. H. W., 1976. Atlas of seismic activity: 1909–1968. *Inst. Geol. Sci., Seis. Bull.* No. 4, HMSO.

Crampin, S. & Uçer, S. B., 1975. The seismicity of the Marmara Sea region of Turkey, *Geophys. J. R. astr. Soc.*, **40**, 269–288.

Davison, C., 1936. *Great Earthquakes*, Thomas Murby & Co., London.

Enescu, D., Marza, V. & Zamarca, I., 1974. Contributions to the statistical prediction of Vrancea earthquakes, *Rev. roum. Geol. Geophys. Geogr., Geophysique*, **18**, 67–79, Bucarest.

Epstein, B. & Lomnitz, C., 1966. A model for the occurrence of large earthquakes, *Nature*, **211**, 954–956.

European Mediterranean Seismological Centre, Working Group of the Friuli Earthquakes, 1976. Revised hypocenters and magnitude determinations of major Friuli shocks, *Friuli Earthquakes Meeting*, Udine, 1976 December 4–5.

Fairhead, J. D. & Girdler, R. W., 1971. The seismicity of Africa, *Geophys. J. R. astr. Soc.*, **24**, 271–301.

Fisher, R. A. & Tippett, L. H. C., 1928. Limiting forms of the frequency distribution of the largest or smallest member of a sample, *Proc. Camb. phil. Soc.*, **24**, 180–190.

Francis, T. J. G. & Porter, I. T., 1971. A statistical study of Mid-Atlantic Ridge earthquakes, *Geophys. J. R. astr. Soc.*, **24**, 31–50.

Franke, A. & Gutdeutsch, R., 1974. Macroseismic estimations of parameters of Austrian earthquakes during the period 1905–1973, *J. Geophys.*, **40**, 173–188, in Austrian.

Galanopoulos, A. G., 1968. On quantitative determination of earthquake risk, *Annali Geofis.*, **21**, 193–206.

Galanopoulos, A. G., 1971. Minimum and maximum magnitude threshold in the area of Attica, Greece, *Annali Geofis.*, **24**, 29–54.

Gaur, V. K. & Chouhan, R. K. S., 1968. Quantitative measures of seismicity applied to Indian regions, *Bull. Indian Soc. Earthq. Tech., Roorkee*, **5**, 63–78.

Gorshkov, G. P., 1961. *Seismicity of Africa*, Unesco, Economic Commission for Africa.

Gouin, P., 1976. Seismic zoning in Ethiopia, *Bull. geophys. Obs., Ethiopia*, No. 17.

Gringorten, I. I., 1963a. A plotting rule for extreme probability paper, *J. geophys. Res.*, **68**, 813–814.

Gringorten, I. I., 1963b. Envelopes for ordered observations applied to meteorological extremes, *J. geophys. Res.*, **68**, 815–826.

Gumbel, E. J., 1945. Floods estimated by probability methods, *Engng News Rec.*, **134**, 97–101.

Gumbel, E. J., 1958. *Statistics of Extremes*, Columbia University Press, New York.

Gutenberg, B. & Richter, C. F., 1954. *Seismicity of the Earth and Associated Phenomena*, Princetown University Press.

Heezen, B. C. & Ewing, M., 1955. Orleansville earthquake and turbidity currents, *Bull. Am. Ass. Petrol. Geol.*, **39**, 2505–2514.

Jenkinson, A. F., 1955. The frequency distribution of the annual maximum (or minimum) values of meteorological elements, *Q. J. R. met. Soc.*, **87**, 158–171.

Kaila, K. L., Gaur, V. K. & Narain, H., 1972. Quantitative seismicity maps of India, *Bull. seism. Soc. Am.*, **62**, 1119–1132.

Kaila, K. L. & Madhava Rao, N., 1975. Seismotectonic maps of the European area, *Bull. seism. Soc. Am.*, **65**, 1721–1732.

Kaila, K. L., Madhava Rao, N. & Narain, H., 1974. Seismotectonic maps of South-West Asia region Comprising Eastern Turkey, Caucasus, Persian plateau, Afghanistan and Hindukush, *Bull. seism. Soc. Am.*, **64**, 657–669.

Kaila, K. L. & Narain, H., 1971. A new approach for preparation of quantitative seismicity maps as applied to Alpide Belt–Sunda Arc and adjoining areas, *Bull. seism. Soc. Am.*, **61**, 1275–1291.

Kanamori, H., 1977. The energy release in great earthquakes, *J. geophys. Res.*, **82**, 2981–2987.

Kanamori, H., 1978. Quantification of earthquakes, *Nature*, **271**, 5644, 411–414.

Kárník, V., 1968. *Seismicity of the European Area, Part I*, Academia, Praha.

Kárník, V., 1971. *Seismicity of the European Area, Part II*, Academia, Praha.

Kárník, V. & Hubnerova, Z., 1968. The probability of occurrence of largest earthquakes in the European area, *Pure appl. Geophys.*, **70**, 61–73.

Kárník, V. & Schenkova, Z., 1978. The third asymptotic distribution in earthquake statistics, *Proc. Symp. Anal. Seismicity and on Seismic Risk*, Liblice, 1977 October 17–22, pp. 335–350, Academia, Prague.

Kimball, B. F., 1960. On the choice of plotting positions on probability paper, *J. Am. statist. Ass.*, **55**, 546–560.

Knopoff, L. & Kagan, Y., 1977. Analysis of the theory of extremes as applied to earthquake problems, *J. geophys. Res.*, **82**, 5647–5657.

Krumbien, W. C. & Lieblein, J., 1956. Geological application of extreme value methods to interpretation of cobbles and boulders in gravel deposits, *Trans. Am. geophys. Un.*, **37**, 313–319.

Latter, J. H., 1970. The interdependence of seismic and volcanic phenomena, *PhD thesis*, University of Edinburgh.

Levenburg, K., 1944. A method for the solution of certain non-linear problems in least squares, *Q. appl. Math.*, **2**, 164–168.

Lilwall, R. C., 1976. Seismicity and seismic hazard in Britain, *Inst. Geol. Sci., Seis. Bull.* No. 4, HMSO.

Lomnitz, C., 1966. Statistical prediction of earthquakes, *Rev. Geophys.*, **4**, 377–393.

Makjanic, B., 1972. A contribution to the statistical analysis of Zagreb earthquakes in the period 1869–1968, *Pure appl. Geophys.*, **95**, 80–88.

Makropoulos, K. C., 1978. The statistics of large earthquake magnitude and an evaluation of Greek seismicity, *PhD thesis*, University of Edinburgh.

Marquardt, D. W., 1963. An algorithm for least-squares estimation of nonlinear parameters, *J. Soc. ind. appl. Math.*, **11**, 431–441.

Marshall, P. D., 1970. Aspects of spectral difference between earthquakes and underground explosions, *Geophys. J. R. astr. Soc.*, **20**, 397–416.

McKenzie, D. P., 1972. Active tectonics of the Mediterranean Region, *Geophys. J. R. astr. Soc.*, **30**, 109–185.

Milne, W. G. & Davenport, A. G., 1969. Distribution of earthquake risk in Canada, *Bull. seism. Soc. Am.*, **59**, 729–754.

Molchan, G. M., Keilis-Borok, V. I. & Vilkovich, G. V., 1970. Seismicity and principal seismic effects, *Geophys. J. R. astr. Soc.*, **21**, 323–335.

Molnar, P. & Tapponnier, P., 1975. Cenozoic tectonics of Asia: Effects of a continental collision, *Science*, **189**, 4201, 419–426.

Nedeljkovic, R. L., 1950. Distribution des intensités maxima des tremblements de terre du territoire Yougoslave 360–1949. *Inst. Seis. Beograd.*

Nordquist, J. M., 1945. Theory of largest values applied to earthquake magnitudes, *Trans. Am. geophys. Un.*, **26**, 29–31.

North, R., 1974. Seismic slip rates in the Mediterranean and Middle East, *Nature*, **252**, 560–563.

North, R., 1977. Seismic moment, source dimensions, and stresses associated with earthquakes in the Mediterranean and Middle East, *Geophys. J. R. astr. Soc.*, **48**, 137–161.

Pastor, A. R., 1927. *Traits Sismiques de la Peninsule Ibérique*, Ateliers de l'Inst. Geogr. Cadastal, Madrid.

Pendse, C. G., 1948. Earthquakes in India and neighbourhood, India Met. Dept., *Scientific Notes*, **10**, 129, 177–220.

Richter, C. F., 1958. *Elementary Seismology*, W. H. Freeman & Co., San Francisco.

Ritsema, A. R., 1967. Mechanisms of European earthquakes, *Tectonophysics*, **4**, 247–259.

Riuscetti, M. & Schick, R., 1975. Earthquakes and tectonics in Southern Italy, *Boll. Geofis. teor. appl.*, **17**, 59–78.

Rothé, J. P., 1969. The seismicity of the Earth 1953–1965, UNESCO.

Schenkova, Z. & Kárník, V., 1970. The probability of occurrence of largest earthquakes in the European area – Part II, *Pure appl. Geophys.*, **80**, 152–161.

Schenkova, Z. & Kárník, V., 1974. Comparison of methods of determining the largest possible earthquakes, *Izv. Phys. Solid Earth*, **11**, 765–769.

Shakal, A. F. & Willis, D. E., 1972. Estimated earthquake probabilities in the North Circum-Pacific area, *Bull. seism. Soc. Am.*, **62**, 1397–1410.

Utsu, T., 1966. A statistical significance test of the difference in b-value between two earthquake groups, *J. Phys. Earth*, **14**, 37–40.

Wilson, A. T., 1930. Earthquakes in Persia, *Bull. Sch. Orient. Studies, London Inst.*, **6**, 103–131.

Yegulalp, T. M., 1974. Forecasting for largest earthquakes, *Mgmt Sci.*, **21**, 418–421.

Yegulalp, T. M. & Kuo, J. T., 1974. Statistical prediction of the occurrence of maximum magnitude earthquakes, *Bull. seism. Soc. Am.*, **64**, 393–414.